© 2016. Published by The Company of Biologists Ltd | Journal of Cell Science (2016) 129, 3832-3844 doi:10.1242/jcs.183541

RESEARCH ARTICLE

Sortilin regulates sorting and secretion of Sonic hedgehog

Charles Campbell[1,2], Shawn Beug[1,3], Philip E. B. Nickerson[4], Jimmy Peng[5,6], Chantal Mazerolle[1], Erin A. Bassett[1], Randy Ringuette[1,2], Fadumo A. Jama[1,3], Carlos Morales[7], Annabel Christ[8] and Valerie A. Wallace[1,3,4,*]

ABSTRACT

Sonic Hedgehog (Shh) is a secreted morphogen that is an essential regulator of patterning and growth. The Shh full-length protein undergoes autocleavage in the endoplasmic reticulum to generate the biologically active N-terminal fragment (ShhN), which is destined for secretion. We identified sortilin (Sort1), a member of the VPS10P-domain receptor family, as a new Shh trafficking receptor. We demonstrate that Sort–Shh interact by performing coimmunoprecipitation and proximity ligation assays in transfected cells and that they colocalize at the Golgi. Sort1 overexpression causes re-distribution of ShhN and, to a lesser extent, of full-length Shh to the Golgi and reduces Shh secretion. We show loss of Sort1 can partially rescue Hedgehog-associated patterning defects in a mouse model that is deficient in Shh processing, and we show that Sort1 levels negatively regulate anterograde Shh transport in axons *in vitro* and Hedgehog-dependent axon–glial interactions *in vivo*. Taken together, we conclude that Shh and Sort1 can interact at the level of the Golgi and that Sort1 directs Shh away from the pathways that promote its secretion.

KEY WORDS: Hedgehog, Sortilin, Trafficking, Secretion, Neuron, Golgi

INTRODUCTION

Sonic Hedgehog (Shh) is a secreted morphogen that activates a highly conserved signal transduction pathway to regulate patterning and proliferation in developing and adult tissues (reviewed in Jiang and Hui, 2008). Mutations in Shh that affect processing or secretion can cause congenital diseases in humans (Maity et al., 2005; Roessler et al., 1996; Schell-Apacik et al., 2003), highlighting the importance of understanding the mechanisms that control trafficking of this morphogen.

Production of biologically active Shh protein requires a complex sequence of post-translational modifications, including cleavage of the Shh signal peptide upon entry into the endoplasmic reticulum (ER) (Lee et al., 1994; Porter et al., 1995), followed by endoproteolysis in the ER that is catalyzed by the Shh C-terminal (ShhC) intein domain, which separates itself from the Shh N-terminal (ShhN) domain and stimulates the addition of a cholesterol molecule to the C-terminus of ShhN (Aikin et al., 2012; Chen et al., 2011; Porter et al., 1996). ShhN is further modified by the addition of a palmitate moiety at the N-terminus (Pepinsky et al., 1998), yielding the mature ligand (ShhNp). Although the majority of full-length Shh is processed to ShhN and ShhC in the ER (Chen et al., 2011; Huang et al., 2013), there is evidence from *Drosophila* studies that a pool of full-length Shh escapes processing and is targeted for secretion (Tokhunts et al., 2010).

After processing, ShhNp is trafficked to the plasma membrane, where the lipid modifications promote association of ShhNp with lipid rafts (Karpen et al., 2001). Various mechanisms exist to facilitate trafficking and the release of Hedgehog (Hh) proteins, including solubilization of monomeric and multimeric Hh mature ligands, incorporation into lipoprotein complexes and exosomes, and cytoneme-mediated transport (reviewed in Briscoe and Thérond, 2013; Guerrero and Kornberg, 2014). Evidently, Shh processing and secretion are highly complex and regulated events, with numerous context-dependent mechanisms existing to deliver ShhNp to its target cells. In order to identify new Shh-interacting proteins that have the potential to regulate Shh trafficking, we performed a GST-affinity screen using Shh as bait and rat brain microsomal fractions as prey. We identified sortilin (Sort1) as a candidate Shh-interacting protein.

Sort1 is a multifunctional sorting receptor of the VPS10P-domain receptor family, which includes family members Sort1, SorLA (also known as SORL1), SorCS1, SorCS2 and SorCS3 (Hampe et al., 2000; Hermey et al., 2003; Jacobsen et al., 1996; Petersen et al., 1997; Rezgaoui et al., 2001). Sort1, the prototypic family member, is involved in targeting ligands, including neurotrophins and neurotrophin receptors, to various intracellular compartments, including the endosomal and regulated secretory pathway (RSP) (Chen et al., 2005; Evans et al., 2011; Vaegter et al., 2011; Yang et al., 2011), and lysosomes (Canuel et al., 2008; Evans et al., 2011; Hassan et al., 2004; Lefrancois et al., 2003; Ni and Morales, 2006; Yang et al., 2013; Zeng et al., 2009). Sort1 also functions as a cell surface receptor for neurotrophins and other growth factors (Nykjaer et al., 2004; Teng et al., 2005). Sort1 is produced as a precursor polypeptide, with a short cytoplasmic tail containing sorting domains (Nielsen et al., 2001); a transmembrane region; the VPS10P ligand-binding domain (Marcusson et al., 1994); and a short N-terminal pro-peptide, which promotes proper folding of the immature peptide and inhibits premature binding of the majority of Sort1 ligands before cleavage by furin in the late trans-Golgi network (TGN) (Hermey et al., 2003; Munck Petersen et al., 1999). The contextually diverse functions of Sort1 in regulating intracellular trafficking of ligands make it an intriguing new receptor for Shh. We probed this interaction using *in vitro* expression of Shh along with various perturbations of Sort1 function in cell lines and primary neuron cultures by examining genetic interactions using Sort1-deficient animals in a sensitized Shh

[1]Regenerative Medicine Program, Ottawa Hospital Research Institute, 501 Smyth Road, Ottawa, Ontario, Canada K1H 8L6. [2]Department of Cellular and Molecular Medicine, University of Ottawa, 451 Smyth Road, Ottawa, Ontario, Canada K1H 8M5. [3]Department of Biochemistry, Microbiology, and Immunology, University of Ottawa, 451 Smyth Road, Ottawa, Ontario, Canada K1H 8M5. [4]Vision Science Division, Krembil Research Institute, University Health Network and Department of Ophthalmology and Vision Sciences, University of Toronto, 60 Leonard Street, Toronto ON M5T 2S8. [5]Department of Biology, McGill University, 1205 Ave Docteur Penfield Room W4/8, Montreal, Quebec, Canada H3A 1B1. [6]Institut de recherches cliniques de Montréal (IRCM), 110 Avenue des Pins Ouest, Montréal, Quebec, Canada H2W 1R7. [7]Department of Anatomy and Cell Biology, McGill University, 3640 Rue University, Montréal, Quebec, Canada H3A 0C7. [8]Max-Delbrück-Center for Molecular Medicine, Robert-Rössle-Str. 10, 13125 Berlin, Germany.

*Author for correspondence (vwallace@uhnresearch.ca)

V.A.W., 0000-0003-3721-9017

Received 18 November 2015; Accepted 26 August 2016

Journal of Cell Science (2016) 129, 3832-3844 doi:10.1242/jcs.183541

system, as well as by manipulating Sort1 function in Shh-dependent tissue patterning *in vivo*. Our results support a model in which Sort1 functions as a trafficking receptor for Shh at the level of the Golgi, directing it away from pathways that promote Shh secretion. This inhibitory role for Sort1 on the secretion of Shh is supported by *in vivo* evidence showing that the Sort1 levels are inversely associated with the levels of Shh-dependent patterning and proliferation.

RESULTS

Sort1 interacts with Shh

To identify new Shh-interacting proteins, we performed a GST-affinity purification screen using ShhN–GST and ShhC–GST as bait and rat brain microsomal fraction, in two different detergent preparations, as prey. Eluted proteins were resolved by performing SDS-PAGE, and unique bands were excised and analyzed by using mass spectrometry analysis. Candidates were filtered based on peptide abundance, and common known sepharose bead contaminants (Kocks et al., 2003; Shevchenko et al., 2002; Trinkle-Mulcahy et al., 2008) and cytosolic proteins were excluded from further analysis. We identified a number of new interacting candidates (Table S1) that were involved in diverse cellular functions, including intracellular sorting, receipt of extracellular ligands and protein maturation. The efficacy of the screen was confirmed by the identification of several known Shh interacting proteins, including low-density-lipoprotein receptor-related protein-1 (Capurro et al., 2012) and glypican-5 (Gpc5) (Li et al., 2011). Interestingly, we identified two members of the sortilin family, Sort1 and SorLA, in ShhC and ShhN pulldowns, respectively (Table S1). We prioritized Sort1 for further studies because of its known function in neuropeptide and receptor anterograde trafficking in neurons (Chen et al., 2005; Evans et al., 2011; Vaegter et al., 2011; Yang et al., 2011), and also because of the reported role for the C-terminus of Hh proteins in axonal trafficking (Huang and Kunes, 1996).

The interaction between Sort1 and Shh was confirmed in co-immunoprecipitation experiments in cells expressing Sort1–Myc–His, epitope-tagged ShhN (ShhN-Fc and ShhN-AP) (Fig. 1A), the N- or C- fragment of Shh tagged with fluorescent protein (ShhEYFP-N or ShhECFP-C, respectively) (Fig. 1B), and full-length Shh (ShhFL), which undergoes processing to generate ShhN and ShhC (Fig. 1C). Sort1–Myc–His interacted with both Shh domains and ShhFL (Fig. 1A–C). These data demonstrate the potential of Sort1 to interact with ShhN and the precursor protein ShhFL. To further validate the interaction between Shh and Sort1 in cells, we compared the subcellular distribution of both proteins in co-transfection experiments. Because the C-terminal epitope tag on full-length Sort1 could affect normal trafficking of the protein, an untagged version of full-length Sort1 was used in these and all subsequent experiments. We transfected COS1 cells with wild-type ShhFL and Sort1 or a C-terminal truncated form of Sort1 (tSort), which lacks trafficking domains and accumulates in the TGN (Chen et al., 2005; Nielsen et al., 2001). Overexpression of Sort1 altered the distribution pattern of Shh from a diffuse reticular pattern to a more compact perinuclear distribution that colocalized with staining of Sort1 (Fig. 1D). Expression of tSort resulted in a more striking perinuclear accumulation of Shh (Fig. 1D), which overlapped with that of a TGN marker (Fig. 1G) but not with that of an ER marker (Fig. 1H), indicating a predominant interaction of tSort with the biologically active ShhN fragment. To address whether the colocalization of Sort1 and Shh was caused by close physical proximity of the proteins, we used an *in situ* proximity ligation assay (PLA). Cells were co-transfected with Shh and Sort1, stained with specific primary antibodies, which was followed by staining with species-specific secondary antibodies conjugated with complementary oligonucleotides (Soderberg et al., 2003, 2008). If the secondary antibodies are within 30 nm, the oligonucleotides can be ligated, amplified and visualized as fluorescent puncta. PLA product was detected in cells that co-expressed Shh and Sort1 (Fig. 1E), and some of the product was localized to the vicinity of the Golgi, based on the distribution of a co-transfected Golgi marker (Fig. 1F). This PLA signal represents physical proximity of the proteins rather than random interactions in the secretory pathway because no PLA signal was detected in cells that had been co-transfected with Shh and BDNF (Fig. 1E,I) or Frizzled4 (Fzd4) and controls (Fig. 1I). These findings indicate that Shh and Sort1 can colocalize to the Golgi and that their interaction is, possibly, direct.

In addition to intracellular protein sorting, a small pool of Sort1 localizes to the plasma membrane where it functions in neurotrophin signaling (Nykjaer et al., 2004; Teng et al., 2005). Thus, we also investigated whether Sort1 expression in Hh-receiving cells would modulate Shh pathway activation. We transfected 3T3 cells with Sort1 or Gpc5, a Shh-binding protein that potentiates Hh signaling (Li et al., 2011), and monitored activation of a Gli-luciferase Hh reporter in response to treatment with recombinant Shh. Sort1 expression had no effect on Shh signaling compared with controls, while expression of Gpc5 strongly enhanced Shh signaling (Fig. 1J). This result suggests that Sort1 interactions with Shh are more relevant to Shh trafficking rather than the response of cells to Shh ligand.

Sort1 promotes the accumulation of Shh in the Golgi and reduces Shh secretion

To identify the intracellular compartments where both Shh and Sort1 interact, we applied subcellular fractionation followed by western blot analysis to compare the distribution of Shh and Sort1 across various subcellular compartments. Briefly, CHO cells, wild-type or stably transfected with Sort1 (CHO-sortilin), were transiently transfected with Shh, and individual fractions were blotted for Shh, Sort1 and compartment-specific markers (Fig. 2). In wild-type CHO and CHO-sortilin cells, similar levels of ShhFL and ShhN were detected in fractions corresponding to the ER [marked by glucose-related protein 78 (GRP-78); fractions 4–6] (Fig. 2A). In contrast, in CHO-sortilin cells, there was enrichment of ShhN, and to a lesser extent of ShhFL, in the Golgi [marked by Golgi SNARE 28 (GS28) and the protein 'vesicle transport through interaction with t-SNAREs homolog 1B' (Vti1b); fractions 7–15]. We do not think that detection of ShhFL in the Golgi is an artifact of overexpression as we achieved comparable levels of Shh protein expression to those observed in other studies (Chen et al., 2011), and previous studies show that full-length Hh can be targeted for secretion in *Drosophila* (Tokhunts et al., 2010). The increase in ShhN in CHO-sortilin cells was particularly strong in later Golgi fractions (fractions 13–14), which overlapped with Sort1. This Golgi retention of ShhN in CHO-sortilin cells was also associated with reduced secretion of ShhN in the culture medium (Fig. 2B). Therefore, because elevated levels of Sort1 retain Shh proteins in the Golgi and reduce Shh secretion, we suggest that Sort1 functions as a sorting receptor that binds to ShhN in the Golgi and directs ShhN away from pathways that destine Shh for secretion.

Sort1 knockout can rescue midline defects in a Shh-processing mutant

Germline Sort1-knockout (*Sort1*$^{-/-}$) is not associated with developmental defects, including phenotypes associated with

Journal of Cell Science (2016) 129, 3832-3844 doi:10.1242/jcs.183541

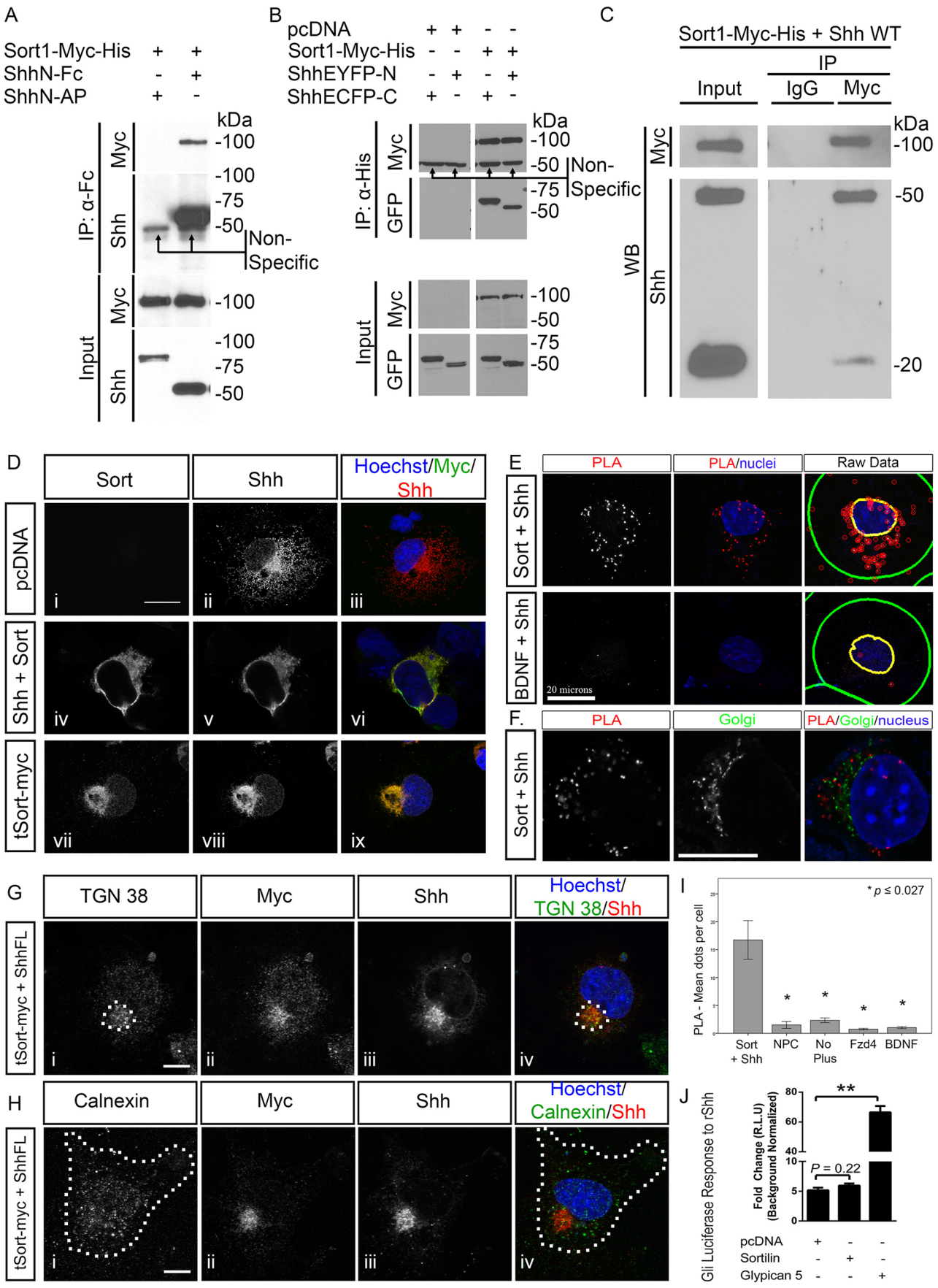

Fig. 1. See next page for legend.

Journal of Cell Science (2016) 129, 3832-3844 doi:10.1242/jcs.183541

Fig. 1. Interaction of Shh and Sort1. (A) Sort1 and Shh co-immunoprecipitation. Lysates from COS cells expressing Fc- (right lane) or AP- (left lane) tagged ShhN along with Sort1–Myc–His were immunoprecipitated (IP) with anti-Fc-antibody-conjugated beads. Immunoprecipitated and input samples were analyzed by western blotting with anti-Hh antibodies (clone H160) to detect Shh (bottom panels) or anti-Myc antibodies to detect Sort1–Myc–His (top panels). (B) Co-immunoprecipitation of Sort1–Myc–His from lysates of COS cells that had been transfected with ShhECFP-C (left lanes) or ShhEYFP-N (right lanes) and with Sort1–Myc–His. Immunoprecipitation and input samples were analyzed by western blotting for Shh (bottom panels) or Sort1–Myc–His (top panels). For A and B, labels indicate non-specific bands that correspond to heavy chain IgG present from the immunoprecipitates. (C) Co-immunoprecipitation of Sort1–Myc–His from lysates of COS cells transfected with ShhFL (Shh WT) and Sort1–Myc–His. Lysates were immunoprecipitated with anti-Myc antibody (right panel, right lane) or species-matched IgG (right panel, left lane). Immunoprecipitates and input samples were analyzed by western blotting for Shh (bottom panels) or Sort1–Myc–His (top panels). (A–C) Representative blots from three independent experiments. (D) Effect of tSort on Shh distribution. Representative immunocytochemistry and Hoechst 33342 nuclear labeling of fixed and permeabilized COS cells expressing ShhFL with pcDNA (i,ii), Sort1 (iv–vi, Sort) or tSort–Myc (vii–ix). (E) PLA on COS cells co-transfected with ShhFL and Sort1, or BDNF as a non-binding control. Raw data representing Blobfinder-mediated quantification of PLA dots. Scale bar: 20 µm. (F) PLA in COS cells co-transfected with Shh, Sort1 and the CellLight Golgi-GFP reporter. Scale bar: 20 µm. (G,H) Representative immunocytochemistry and Hoechst 33342 nuclear staining on fixed and permeabilized COS cells expressing ShhFL and tSort-Myc. Dashed lines indicate extent of TGN (G, marked by TGN-38) or ER staining (H, marked by calnexin). Images are representative from three independent experiments. Scale bar: 10 µm. (I) A quantification of cytoplasmic PLA dots in a minimum of 100 cells per group using Blobfinder algorithms. Data represent mean±s.e.m. Analyzed by using ANOVA and Scheffé's post hoc comparisons. (J) Sort1 expression in receiving cells does not affect signal transduction in response to exogenous Shh. Gli-luciferase activity in serum-starved 3T3 cells transfected with the indicated expression vectors and treated with recombinant Shh for 24 h. Bars indicate mean Gli-luciferase activity normalized to constitutive *Renilla*-luciferase expression (n=3 independent experiments per condition)

altered Hh signaling (Jansen et al., 2007; Zeng et al., 2009). Therefore, to examine whether Sort1 function impacts Shh processing *in vivo*, we examined its effect in a sensitized system using a processing-deficient Shh-mutant mouse model, Shh::GFP (Chamberlain et al., 2008). The Shh::GFP knockin allele is processed inefficiently owing to the insertion of a fluorescent tag in the N-terminal domain of the protein (Fig. 3A) (Chamberlain et al., 2008). Consistent with this processing defect, homozygosity for the Shh::GFP allele ($Shh^{GFP/GFP}$) is embryonic lethal, and is characterized by craniofacial deformities and cyclopia due to loss of Shh function (Chamberlain et al., 2008). Previous work has shown that eye-field defects observed in Shh-deficient mice, including the Shh::GFP model, can be rescued by increasing Hh signaling by reducing the gene dosage of Hh pathway antagonists (Chamberlain et al., 2008; Litingtung and Chiang, 2000). Because Sort1 reduces Shh secretion *in vitro*, and Sort1 is expressed in the ventral midline at the stage of Shh-mediated patterning (Hermans-Borgmeyer et al., 1999), we reasoned that loss of function for Sort1 would ameliorate some of the Hh-associated defects in $Shh^{GFP/GFP}$ mice. We first addressed whether Sort1 knockdown altered the secretion of ShhEYFP-N *in vitro*. We used small hairpin (sh)RNA constructs to generate stable PC12 cell lines that had Sort1 knockdown (Fig. S1), transfected them with ShhEYFP-FL and measured the concentration of ShhEYFP-N in cell supernatants by western blot and ELISA (Fig. 3A). Here, we found that levels of secreted ShhEYFP-N were increased in Sort1-knockdown cells compared to those in control PC12 cells (Fig. 3A). Next, we generated $Shh^{GFP/GFP}$ animals on wild-type or Sort1-mutant backgrounds ($Sort1^{+/+}$ versus $Sort1^{-/-}$) and compared the width of the eye field at embryonic day (E)14.5, an age at which bilateral separation of the eye field is readily apparent in wild-type animals (Fig. 3Bi). Remarkably, the optic-field width [as confirmed by neural retina marker *Vsx2* expression (Fig. 3Bii)] was significantly increased in $Shh^{GFP/GFP}$;$Sort1^{-/-}$ mice compared with $Shh^{GFP/GFP}$;$Sort1^{+/+}$ controls (Fig. 3Biii, Biv and B′). However, we did not observe full bilateral separation of the eye field that was comparable to that in $Shh^{+/GFP}$ mice (Fig. 3Bi and B′), indicating that there was not full rescue of Hh signaling in the compound mutants, which is also consistent with the failure to restore Hh target gene expression in the ventral midline in the compound mutant animals (data not shown). These data are consistent with the interpretation that Sort1 exerts an inhibitory effect on Shh secretion *in vivo* such that Sort1 deficiency results in a partial rescue of midline defects associated with defective Shh secretion (summarized in Fig. 3C).

Sort1 reduces trafficking of Shh to the RSP

In some projection neurons of the central nervous system (CNS), Shh processing and lipid modification is required for targeting to the RSP (Beug et al., 2011; Petralia et al., 2011) and for activity-dependent secretion (Beug et al., 2011). Because Sort1 affects Shh trafficking and secretion in non-neuronal cell lines, we next investigated how Sort1 affects Shh targeting to the RSP in primary neurons. In primary rat retinal ganglion cells (RGCs), which express endogenous Shh and Sort1 (Fig. 4A), Shh and Sort1 exhibited low levels of colocalization in the soma and the axon (Fig. 4A and A′). We observed a similar distribution and colocalization pattern between endogenous Sort1 and transfected Shh in primary cortical neurons, confirming the efficacy of these neurons in subsequent Sort1 perturbation studies (Fig. S2A). We next examined the effect of Sort1 knockdown on Shh axonal targeting by examining two different pools of axonal Shh – extracellular (where it accumulates on lipid rafts on the plasma membrane) and intracellular (where it is associated with regulated secretory vesicles), which both require proper Shh trafficking (Beug et al., 2011). When we compared the distribution of Shh in cortical neurons as a function of Sort1 expression, we found an inverse relationship between Sort1 expression and the levels of Shh in the axon (Fig. 4; Fig. S3). RNA interference (RNAi)-mediated knockdown of Sort1 with two shRNA constructs in cortical neurons (shSort1A and shSort1B, validation shown in Fig. S1) increased the colocalization of Shh with synaptic vesicle glycoprotein 2A (SV2)+ RSP vesicles and extracellular Shh (Fig. 4C) in axons. We observed similar effects on Shh distribution in cortical neurons from $Sort1^{-/-}$ mice (Fig. 4D; Fig. S3). Re-introduction of Sort1 expression in $Sort1^{-/-}$ neurons significantly reduced Shh levels in the axons (Fig. 4E; Fig. S3), and reduced, albeit not significantly, colocalization of Shh with SV2+ vesicles (Fig. 4E; Fig. S3), suggesting that the effect was specific to loss of Sort1. The effect of Sort1 on Shh distribution in the axon was specific to Shh, as Sort1 knockdown had the opposite effect on hemagglutinin (HA)-tagged BDNF distribution, abolishing axonal trafficking (Fig. S4A), consistent with Sort1 directing BDNF–HA to the axon (Chen et al., 2005). There was no apparent redirection of Shh from other subcellular compartments because colocalization of Shh with lysosomal or endosomal markers was unchanged in $Sort1^{-/-}$ neurons (Fig. S4B). Conversely, increased Sort1 expression in wild-type cortical neurons reduced the extent of the Shh–SV2 colocalization in the axon and the level of extracellular Shh on the axon (Fig. S2B,C). Sort1 overexpression did not alter the total level of SV2+ vesicles in the axons (Fig. S4C), indicating that

Journal of Cell Science (2016) 129, 3832-3844 doi:10.1242/jcs.183541

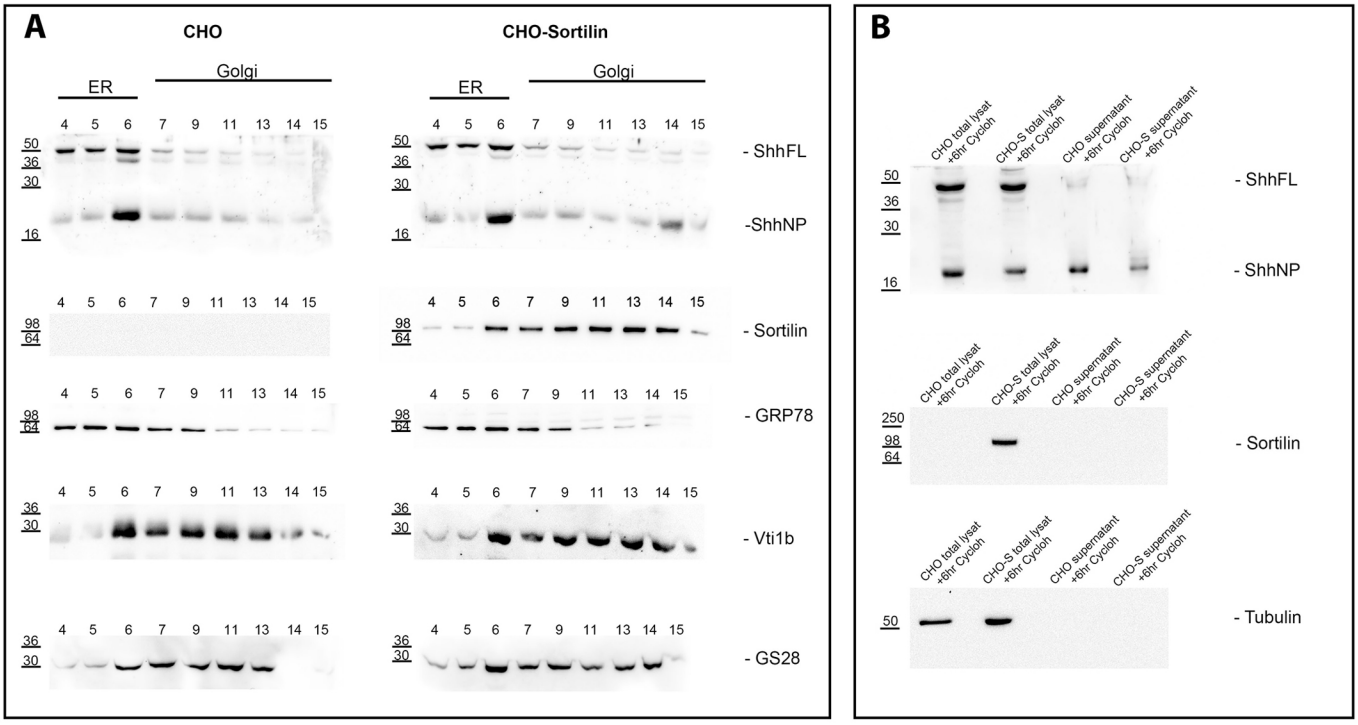

Fig. 2. Sort1 regulates trafficking of ShhN in CHO cells. (A) Wild-type CHO cells and CHO cells that had been stably transfected with an expression construct encoding murine Sort1 were subjected to subcellular fractionation followed by immunodetection of Shh, Sort1 (sortilin), as well as markers Grp78 (ER), Vti1b and GS28 (Golgi). In both cell lines, ShhFL was mainly found in the ER (fractions 4–6), whereas ShhN was detected in the Golgi fractions (fractions 7–15). However, in Sort1-expressing cells, accumulation of ShhN as well as residual levels of ShhFL (fractions 13 and 14) are obvious in the Golgi fractions, overlapping with Sort1+ fractions. (B) Wild-type CHO cells and CHO-sortilin cells were treated for 6 h with cycloheximide (Cycloh). Subsequently, levels of Shh in cell lysate (lysat) and cell supernatant were quantified by western blotting. Both cell lines produced comparable levels of intracellular Shh protein (compare lanes 1 and 2). However, the amount of ShhN released was lower in CHO-sortilin cells compared to that in control cells (compare lanes 3 and 4).

the effect of Sort1 on axonal Shh was not secondary to a general perturbation of biogenesis or trafficking of SV2+ vesicles in the axon. These results are consistent with the notion that Sort1 inhibits Shh targeting to axons and SV2+ vesicles, which is independent of trafficking to the lysosome or endosome, and is independent from its regulation of BDNF trafficking in axons.

Truncated Sort1 perturbs trafficking of endogenous Shh in RGCs, resulting in decreased astrocyte proliferation in the optic nerve

We next investigated the requirement for Sort1 trafficking in neuron-derived Shh signaling *in vivo*. We focused on RGCs, the axons of which project from the retina through the optic nerve to targets in the brain. In addition to its short-range effects in the regulation of proliferation of adjacent neural progenitor cells in the retina (Wang et al., 2005), Shh is also transported down RGC axons, where it is released in the optic nerve to stimulate astrocyte proliferation and oligodendrocyte precursor cell migration (Dakubo et al., 2003, 2008; Soukkarieh et al., 2007; Wallace and Raff, 1999). To perturb Sort1 trafficking, we used an overexpression approach *in vivo*. In control experiments, we determined that tSort expression in cortical neurons caused severe impairment of Shh axonal targeting (Fig. 5A,A′). Consistent with inhibiting RSP targeting, tSort expression in differentiated PC12 cells [which differentiate into a neuronal phenotype that has neuron-like processes and activity-dependent RSP secretion of neuropeptides (Greene and Tischler, 1976)] resulted in a decrease in activity-dependent Shh secretion relative to control conditions (Fig. 5B), consistent with an antagonistic role for tSort in stimulated Shh secretion.

We next asked whether tSort expression in embryonic RGCs *in vivo* affects Shh-dependent proliferation in the optic nerve and retina. Control or tSort expression vectors were co-transfected with YFP into the eye at E13.5 by performing *in utero* electroporation, and the tissue was harvested at E15.5 after a 2-h pulse with 5-ethynyl-2′-deoxyuridine (EdU) to label cells in S-phase (schematic in Fig. 6A). Transfection of RGCs was confirmed by the presence of YFP in the cell bodies located in the retina and axons in the optic nerve (Fig. 6B). At this stage, the majority of the cells in the optic nerve are Pax2+ astrocyte precursor cells (Fig. 6C), which are not electroporated in this procedure. Remarkably, the proportion of EdU+ nuclei in the optic nerve was significantly reduced in samples into which tSort had been electroporated intraocularly relative to that in the control (Fig. 6Bi–Bviii and B′). The proportion of EdU+ cells in the retina of tSort-electroporated animals was also reduced relative to control conditions, albeit not significantly (Fig. 6Bix–Bxvi and B″). This effect of tSort expression on proliferation was restricted to glial cells in the optic nerve, as proliferation of mesenchymal cells located adjacent to the nerve was unaffected (Fig. 6B″). Because we observed YFP+ axons and Pax2+ glial cells in the optic nerve (Fig. 6B,C), we ruled out RGC cell death and impaired astrocyte development as alternative interpretations for the tSort-dependent reduction in astrocyte proliferation. Taken together, these findings indicate that tSort expression in the retina exerts a distal non-cell autonomous effect in the optic nerve. Because Shh is the only reported anterograde signal that controls astrocyte proliferation in the optic nerve (reviewed in Tao and Zhang, 2014), our findings are also consistent with the interpretation that tSort interferes with Shh signaling in the axon.

Journal of Cell Science (2016) 129, 3832-3844 doi:10.1242/jcs.183541

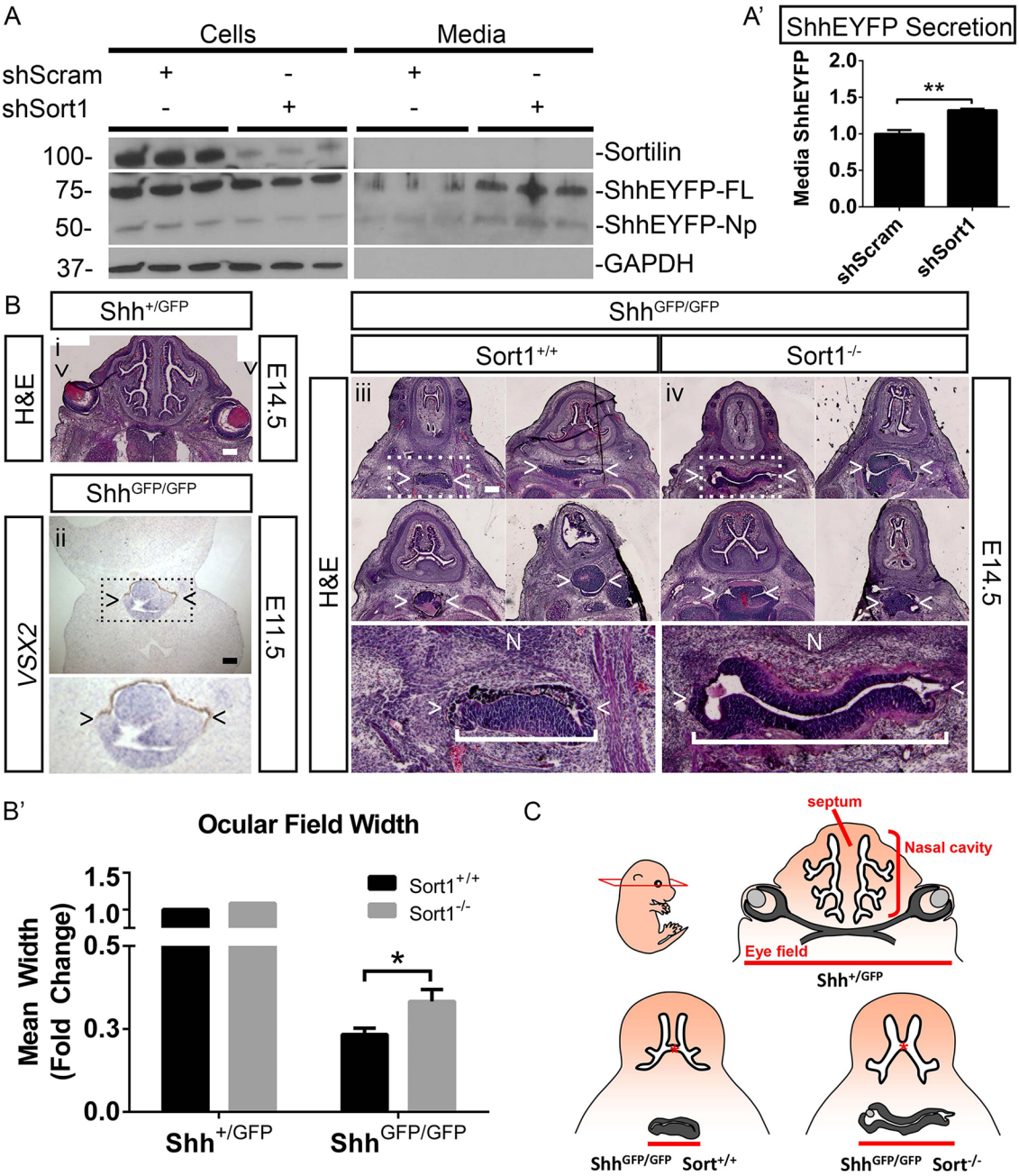

Fig. 3. Impact of Sort1 loss-of-function on processing and patterning using processing-deficient Shh mutants. (A,A′) Sort1 knockdown (shSort1) increases Shh secretion. PC12 cells stably expressing Sort1 or scrambled (shScram) shRNA interference constructs were transfected with the full-length Shh-EYFP fusion reporter ShhEYFP-FL, and cell lysates and culture supernatants were blotted for Sort1, YFP (to detect the Shh constructs) and GAPDH (A). (A′) The concentration of ShhEYFP-N in cell culture supernatants was measured by using an ELISA and were normalized to the total amount of EYFP-tagged Shh (ShhYFP-FL+ ShhEYFP-N) in cell lysates (n=3 independent experiments per condition), error bars represent s.e.m.; *P<0.05, Student's t-test. (B,B′) Sort1 knockout is associated with an increase in eye-field width in the $Shh^{GFP/GFP}$ homozygous mutant. Hematoxylin and eosin (H&E) staining in horizontal sections at the level of the eye field of mouse heads of $Shh^{GFP/GFP}$ mice on wild-type and Sort1-knockout backgrounds at E14.5. Wild-type animals exhibited proper bilateral symmetry of the eyes (i). *In situ* hybridization in coronal sections of $Shh^{GFP/GFP}$ brains confirms the location of a central *Vsx2*+ single eye at the midline (ii). Examples from four mice per genotype are shown, and lower panels are higher magnification images corresponding to the regions indicated in the dashed boxes (iii and iv). > < indicates the location of eye field; N, nasal cavity to indicate the orientation of the tissue; white bracket indicates the width of the eye field. Scale bars: 100 µm. (B′) A quantification of mean eye-field width in compound $Shh^{+/GFP};Sort1^{+/+}$ (n=2), $Shh^{+/GFP};Sort1^{-/-}$ (n=2), $Shh^{GFP/GFP};Sort1^{+/+}$ (n=6) and $Shh^{GFP/GFP};Sort1^{-/-}$ (n=5) mice at E14.5. Serial sections were taken of the eye field for each genotype, and the eye field was measured at its widest point therein. Data were normalized to the values from $Shh^{GFP/GFP};Sort1^{+/+}$ *mice*. Error bars represent s.e.m.; *P<0.05, Student's t-test. (C) Schematic showing plane of section and landmarks used for the analysis of H&E-stained sections.

DISCUSSION

Our study provides the first evidence of a role for Sort1 in modulating Shh trafficking in cell lines and primary neurons. Sort1 can interact with unprocessed, as well as processed, ShhN and ShhC peptides, and overexpression of Sort1 alters the distribution of Shh, retaining it in the Golgi compartment and inhibiting its secretion.

Journal of Cell Science (2016) 129, 3832-3844 doi:10.1242/jcs.183541

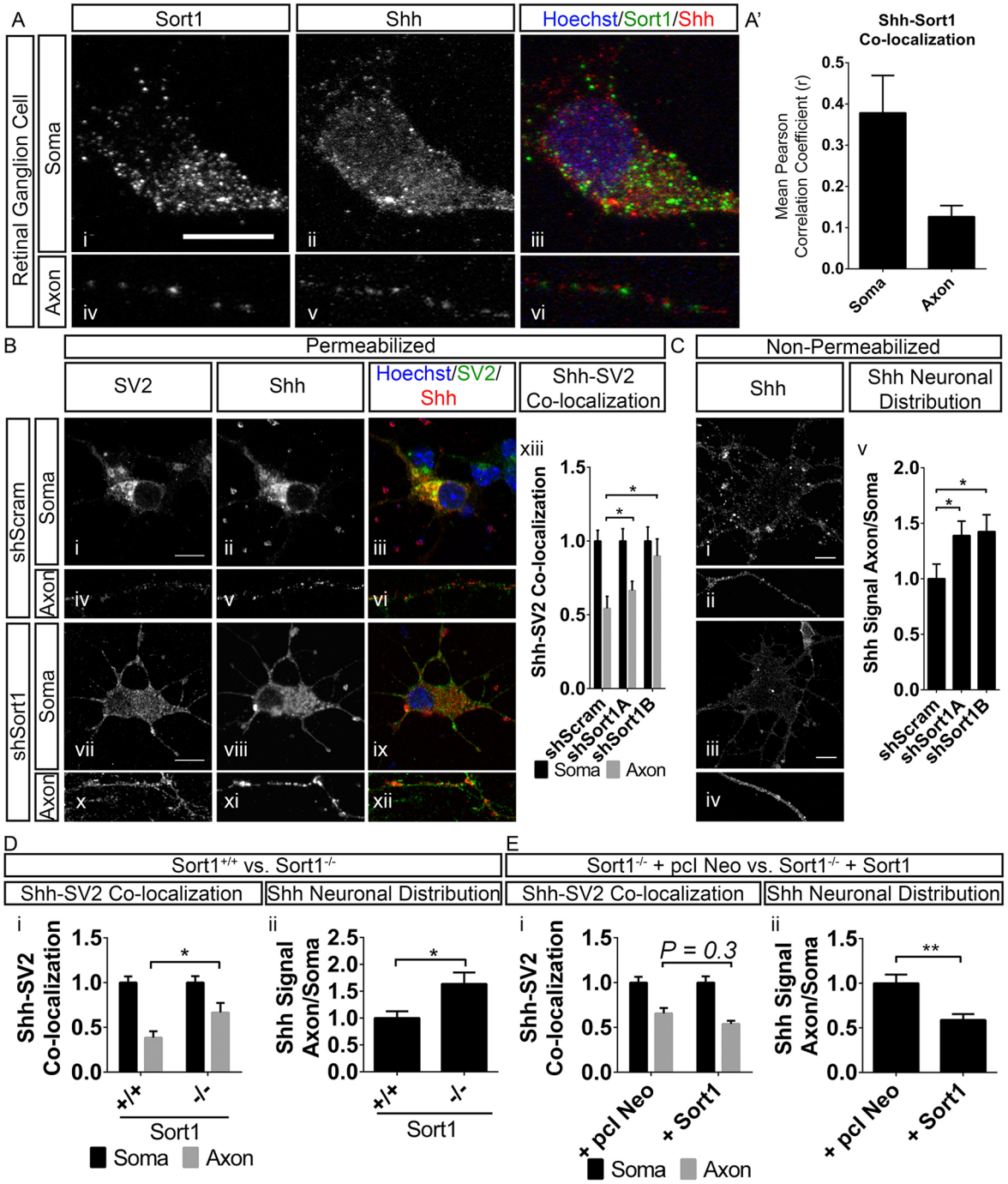

Fig. 4. Sort1 expression negatively correlates with Shh distribution in axons. (A,A′) Shh and Sort1 distribution in the somatodendritic and axonal compartments of primary RGCs. Panels show 1-µm optic sections in the somatodendritic (upper) or axonal (lower) compartments. Scale bar: 10 µm. (A′) Quantification of the colocalization of Shh and Sort1 in the indicated subcellular compartment in RGCs. Graph shows mean Pearson's correlation coefficient (r) (n=5 cells per condition). Error bars represent s.e.m. (B) Knockdown of Sort1 (shSort1) increased the colocalization of Shh with SV2. Representative immunocytochemistry and Hoechst 33342 nuclear staining on fixed and permeabilized primary cortical neurons expressing Shh and a scrambled shRNA (shScram, i–vi) or shSort1 (vii–xii). Panels show 1-µm optic sections in the somatodendritic (upper) or axonal (lower) compartments. Scale bars: 10 µm. Colocalization of Shh and SV2 was quantified using the intensity correlation analysis function in ImageJ (xiii). Bars indicate mean Pearson's correlation coefficient (r) (n=20 neurons per condition) normalized to control values. Error bars represent s.e.m.; *P<0.05, Student's t-test. (C) Knockdown of Sort1 correlates with an increased ratio of Shh signal on the surface of the axon relative to that on the soma. Representative immunocytochemistry analysis on fixed non-permeabilized primary cortical neurons expressing Shh and shScram (i–ii) or shSort1B (iii–iv). Panels show 1-µm optic sections in the somatodendritic (upper) or axonal (lower) panels. Scale bars: 10 µm. The Shh distribution was quantified as the ratio of Shh signal intensity in a distal region of the axon relative to the signal intensity in the soma (v). Graph shows the mean ratio of axon:soma Shh signal (n=20 neurons per condition) normalized to control conditions. Error bars represent s.e.m.; *P<0.05, Student's t-test. (D,E) Increased Shh colocalization with SV2 and an increase in the ratio of Shh signal in the axon relative to that in the soma in transfected primary cortical neurons from *Sort1*$^{-/-}$ mice (D), whereas Sort1 expression in primary cortical neurons from *Sort1*$^{-/-}$ mice rescues the Shh phenotype. (Di,Ei) Colocalization analysis of Shh and SV2 from images in Fig. S2, and (Dii,Eii) Shh neuronal distribution analysis of images shown in Fig. S3. Parameters measured as stated above, n=20 neurons per condition. *P<0.05, **P<0.01, Student's t-test.

Journal of Cell Science (2016) 129, 3832-3844 doi:10.1242/jcs.183541

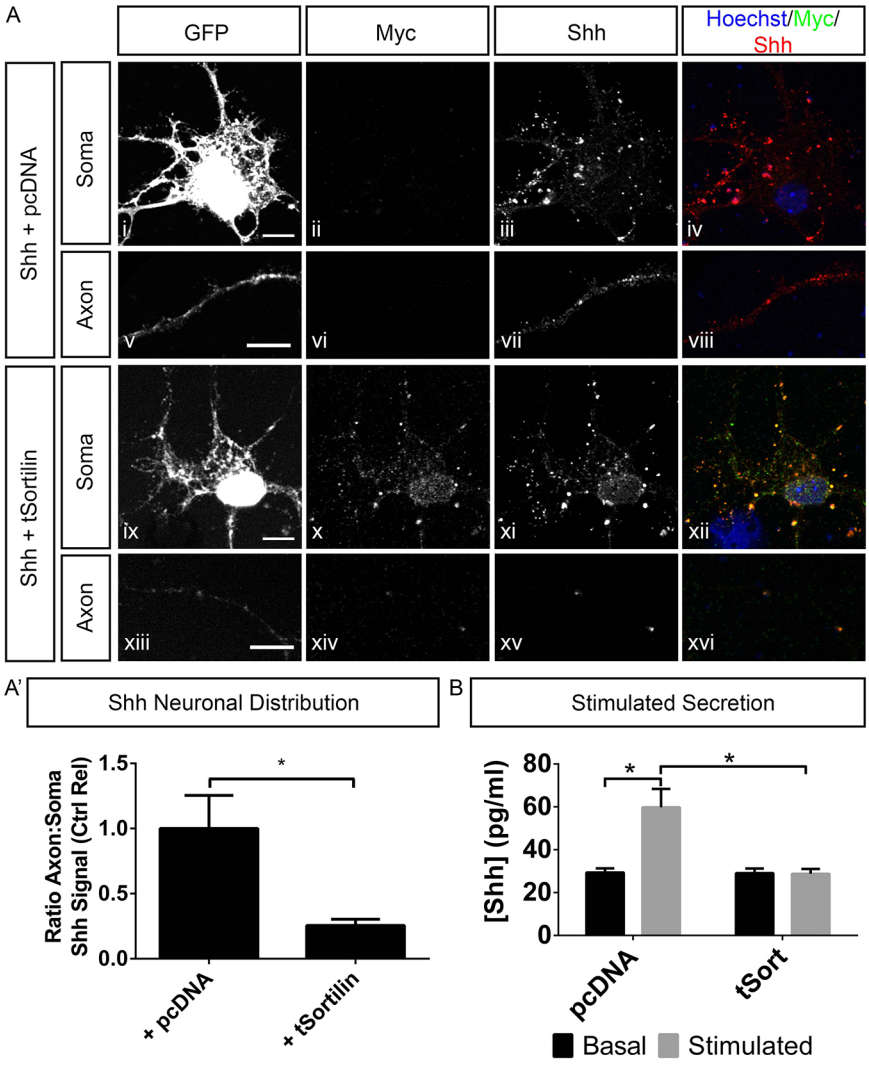

Fig. 5. Sort1 reduces Shh axonal targeting and stimulated secretion. (A) Representative immunocytochemistry and Hoechst 33342 nuclear labeling of permeabilized primary cortical neurons that overexpressed Shh and pcDNA (i–vi) or tSort–Myc (vii–xii), with YFP as a transfection control. Panels show 1-µm optic sections in the somatodendritic (upper) or axonal (lower) compartments. Scale bars: 10 µm. (A′) Shh neuronal distribution quantified as the ratio of Shh signal intensity in a distal region of the axon relative to signal intensity in the soma (v). Graph shows the mean ratio of axon:soma Shh signal (n=20 neurons per condition) relative to that under control conditions. Error bars represent s.e.m.; *P<0.05, Student's t-test. (B) tSort overexpression inhibits Shh stimulated secretion from PC12 cells. Differentiated PC12 cells that stably overexpressed pcDNA or tSort–Myc and had been transiently transfected with ShhFL were exposed to basal or depolarizing conditions, and the concentration of Shh in the medium was quantified by performing an ELISA (n=3 independent experiments per condition); error bars represent s.e.m.; *P<0.05, Student's t-test.

Taken together, these data are consistent with a model in which Sort1 acts as a sorting receptor for Shh in the Golgi to direct it away from pathways that promote Shh secretion. Consistent with this model, loss of Sort1 partially rescued Hh-dependent eye-field defects in an Shh-processing-deficient mutant *in vivo*. Furthermore, Sort1 levels were inversely correlated with polarized trafficking and secretion of Shh *in vitro*, and Sort1 trafficking was required for axon-dependent effects on glial proliferation *in vivo*.

Shh-mediated tissue patterning begins with the production and processing of the full-length precursor protein (Lee et al., 1994; Pepinsky et al., 1998; Porter et al., 1995, 1996), whereupon mature ShhNp is secreted in a short and long range manner through a number of mechanisms (Briscoe and Thérond, 2013; Callejo et al., 2011; D'Angelo et al., 2015; Gradilla et al., 2014; Guerrero and Kornberg, 2014; Matusek et al., 2014; Parchure et al., 2015; Vyas et al., 2014). In neurons, Shh utilizes the RSP as a mode of anterograde transport in axons (Beug et al., 2011); therefore, our identification of Sort1 from a GST-affinity screen provided a candidate sorting receptor for Shh. Our data suggest that the interaction between Shh and Sort1 occurs largely in the TGN, based on colocalization and cellular fractionation studies. This is an interesting new concept that supports Sort1 function in regulating the intracellular fate of ShhN. Identifying other Sort1-mediated trafficking pathways for Shh, including a possible role in the recycling of the morphogen, will be an interesting direction for future studies.

The newly identified role for Sort1 as a regulator of Shh secretion led us to predict that Sort1-knockout animals would exhibit Shh gain-of-function phenotypes, because in the absence of Sort1, more Shh would be directed to secretion pathways. However, germline knockout of Sort1 is not associated with gross phenotypic changes in Hh-dependent tissues. This is not unanticipated because Sort1 knockout is associated with subtle phenotypes that do not impact development (Vaegter et al., 2011); for example, Sort1-knockout mice have no overt neurotrophic phenotypes despite its known roles in neurotrophin receptor trafficking. However, Sort1 knockout aggravates neurotrophic phenotypes when crossed on to a sensitized background – p75 neurotrophin receptor knockout (Vaegter et al., 2011). Moreover, endogenous Shh-responsive systems are sensitive to low concentrations of the ligand, as evidenced by the viability of the Shh heterozygous knockout (Chiang et al., 1996). Finally, our screen identified SorLA as another potential new interacting partner of Shh; therefore, there could be compensatory effects mediated by SorLA upon loss of Sort1. Thus, it is possible that any Hh-like phenotypes in Sort1-knockout animals are masked by a combination of compensatory activity from sortilin-family members and the sensitivity of the system to a range of Shh ligand concentrations.

Journal of Cell Science (2016) 129, 3832-3844 doi:10.1242/jcs.183541

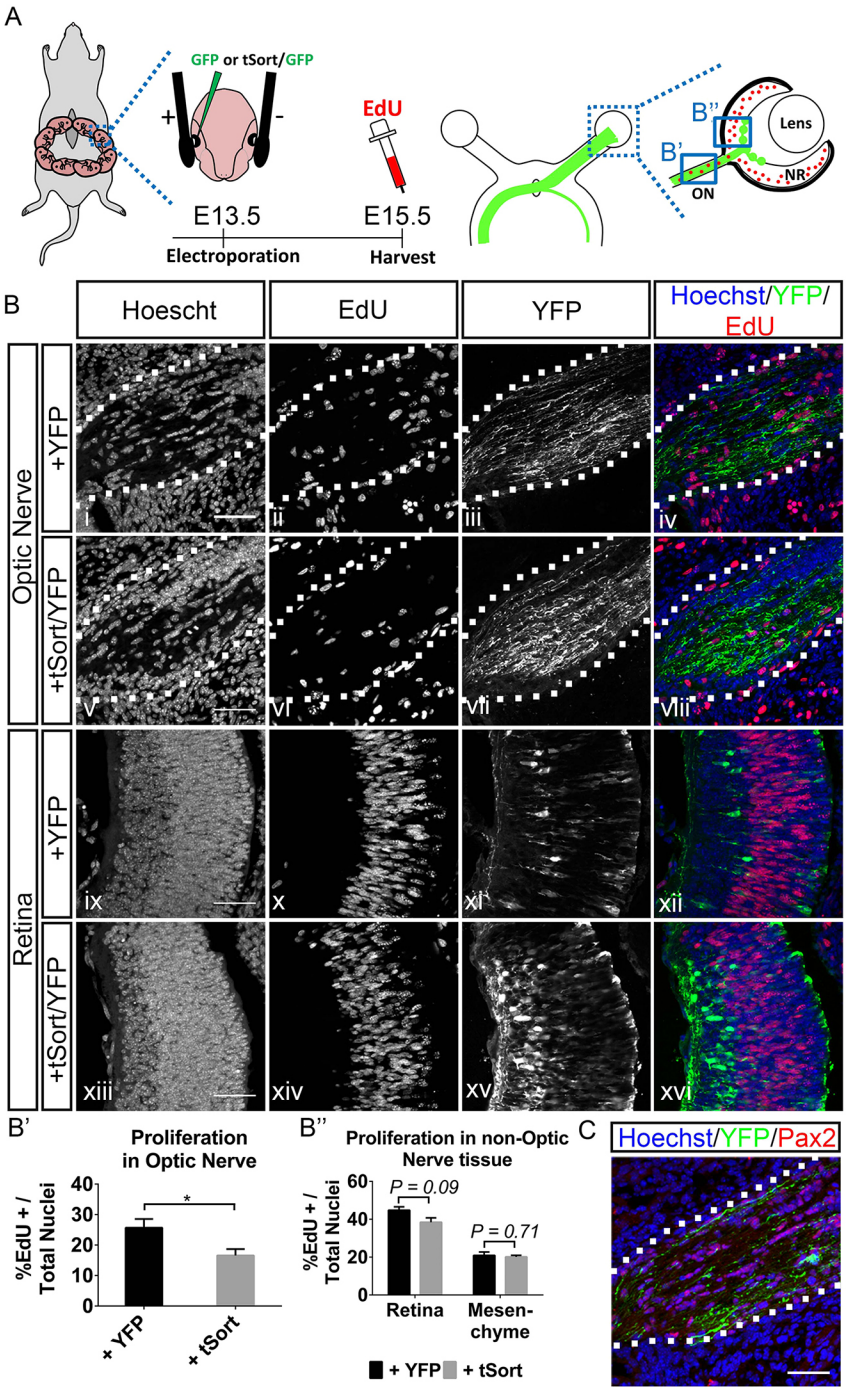

Fig. 6. tSort–Myc expression in the retina affects astrocyte proliferation in the optic nerve. (A) Schematic of the *in utero* electroporation technique. Embryonic mice were electroporated *in utero* at E13.5 with YFP or YFP and tSort–Myc, and harvested at E15.5 (with EdU S-phase labeling 1 h before death). Horizontal sections of the head were used to image the retina and optic nerve. Boxes represent the regions that were used for quantification of EdU. (B) Representative EdU staining, which marks cells in S-phase and Hoechst 33342 nuclear labeling in sections of the optic nerve (outlined by dashed lines) (i–viii) and retina (ix–xvi) of transfected eyes. YFP, a co-transfection marker, marks transfected cells in the retina and transfected axons in the optic nerve. Scale bars: 50 µm. (B′,B″) Bars represent the percentage of EdU+ nuclei as a function of total nuclei in the YFP+ region of the optic nerve (B′) or retina (B″), or in an adjacent mesenchymal region (B″) (YFP, n=4 animals; tSort, n=3 animals). Error bars represent s.e.m., *P<0.05, Student's t-test. (C) Immunohistochemistry analysis for optic nerve Pax2 expression (which marks astrocytes) and Hoechst 33342. YFP marks axons of transfected RGCs, and Pax2 marks astrocyte precursor cells. Scale bar: 50 µm.

We have therefore investigated genetic interactions between Sort1 and the Hh pathway using sensitized *in vivo* models of Hh signaling. Loss of Sort1 has no impact on the incidence or latency of medulloblastoma in Ptch$^{+/-}$ mice (Goodrich et al., 1997), which is dependent on Shh pathway over-activation (C.C. and V.W., unpublished observations). However, reducing Sort1 levels in the context of Shh::GFP homozygosity, characterized by midline defects due to deficient Shh processing, improved eye-field patterning, an Shh-regulated process. The rescue was incomplete, as shown by the lack of expression of midline target genes that require the highest dose of Shh (C.C. and V.W., unpublished observations), indicating that Sort1 knockout does not fully restore Shh signaling.

We have previously reported that Shh is trafficked to the RSP in primary neurons (Beug et al., 2011). Our observation that Sort1 levels negatively correlate with those of Shh in the axon is consistent with the hypothesis that Sort1 also functions in directing Shh away from the RSP pathway. This is notably different from Sort1-dependent anterograde trafficking of BDNF and TRK receptor to axons and to the RSP (Chen et al., 2005; Evans et al., 2011; Vaegter et al., 2011; Yang et al., 2011). This suggests the possibility that Sort1 is the RSP receptor for BDNF and TRK receptors but there exists an additional, as yet unidentified, receptor that likewise regulates Shh targeting to the RSP.

Optic nerve axons have been shown to promote survival of oligodendrocytes and the proliferation of oligodendrocyte precursor

cells and astrocytes (Barres et al., 1993; Barres and Raff, 1993; Burne and Raff, 1997). Shh is the only signal that has been identified to date that mediates the effects of axons on astrocyte proliferation (Dakubo et al., 2008; Wallace and Raff, 1999). We showed that ectopic expression of tSort in RGCs induces a non-cell autonomous effect on astrocyte proliferation in the optic nerve. Thus, in addition to its role in regulating RGC survival in development and in injury models (Lebrun-Julien et al., 2010; Nakamura et al., 2007), our study identifies a second function for Sort1 in axon–glial-cell communication. Our findings also raise the interesting possibility that Sort1 function extends to other aspects of optic nerve biology, including oligodendrocyte development and myelination.

Taken together, we have newly identified an interaction between Sort1 and Shh, wherein Sort1 regulates trafficking of ShhN to the secretory pathway and thereby influences the bioavailability of Shh. This interaction has implications for Shh signaling in developing tissues, including neuroepithelial cells at the CNS midline, and in polarized trafficking of the protein in projection neurons. Considering the ubiquitous expression of Sort1 in known Shh-producing cells, it is possible that Sort1 could regulate Shh-mediated patterning in additional tissues not studied here.

MATERIALS AND METHODS

DNA constructs

Shh-FL, ShhEYFP-FL, ShhEYFP-N and ShhECFP-C constructs were prepared as previously described (Beug et al., 2011). Full-length Shh cDNA (Genbank accession no. NM_009170) was used to generate GST fusion constructs. Shh-N (amino acids 25–198) and Shh-C (amino acids 199–437) were amplified by using PCR and subcloned into the GST recombinant vector pGEX-4T-1 (GE Healthcare) to generate GST–ShhN and GST–ShhC, respectively. pEF, pEF-Sort1 cDNAs were gifts from Dr Peder Madsen (Aarhus University, Aarhus, Denmark). Sort1 was obtained from the IMAGE Consortium and subcloned into pcDNA3.1myc-His(-)C by performing PCR amplification. tSort–Myc was a gift from Dr Carlos Morales (McGill University, Montreal, Québec) and was subcloned into the pCAGGS vector for the electroporation studies. Glypican-5-FLAG was tagged with 3×FLAG upstream of the cleavage site, and subcloned into pcDNA3. BDNF–HA was a gift from Dr Francis Lee (Cornell University, Ithaca, NY). Short hairpin constructs targeting Sort1 were obtained from OriGene. *Renilla*–luciferase was a gift from Dr Alan Mears (Children's Hospital of Eastern Ontario, Ottawa, ON), Gli-responsive luciferase reporter construct was a gift from Dr Hiroshi Sasaki (Osaka University, Osaka, Japan).

GST-affinity purification

Microsomal fractions were obtained from rats at postnatal days 2–3 as follows. Brains were Dounce homogenized in SIM buffer (250 mM sucrose, 5 mM imidazole, 1 mM $MgCl_2$, pH 7.4), centrifuged at 10,000 ***g*** for 30 min, and the supernatant was centrifuged at 100,000 ***g*** for 60 min. The pellet was resuspended in SIM buffer and centrifuged at 100,000 ***g*** for 60 min. The resulting pellet represented the microsomal fraction and was solubilized with either 0.5% CHAPS or NP-40 in 20 mM HEPES-KOH pH 7.4, 150 mM NaCl, 1 mM $MgCl_2$ and clarified by centrifugation at 20,000 ***g*** for 30 min. Solubilized microsomes were precleared through incubation with glutathione-coupled Sepharose beads (GE Healthcare). The precleared fraction was incubated with equimolar amounts of GST, GST–ShhN or GST–ShhC coupled to glutathione-bound beads. Beads were washed sequentially with buffer (20 mM HEPES-KOH, pH 7.4), high-salt buffer (20 mM HEPES-KOH pH 7.4, 300 mM NaCl), detergent buffer (20 mM HEPES-KOH pH 7.4, 300 mM NaCl and 0.1% CHAPS or NP-40) and PBS. Bound proteins were eluted by cleavage with thrombin (GE Healthcare) and resolved on precast 8–16% SDS-PAGE gels (Bio-Rad). Gels were silver stained, and bands were excised and identified by performing mass spectrometry using Qstar and LTQ mass spectrometers (Ottawa Institute of Systems Biology, Ottawa, ON).

Cell culture and transfection

COS-1 (American Type Culture Collection) and 3T3 (American Type Culture Collection) fibroblasts were maintained in Dulbecco's modified Eagle's medium (DMEM) (Life Technologies) supplemented with 10% fetal bovine serum (FBS). PC-12 cells (American Type Culture Collection) were maintained in RPMI-1640 (Life Technologies), supplemented with 10% horse serum, 5% FBS, 2 mM L-glutamine, and 1× penicillin-streptomycin. For differentiation, PC-12 cells were plated on collagen-IV-coated (Sigma) plates (20 µg/cm^2) in RPMI-1640 supplemented with 1% horse serum, 0.5% FBS, 2 mM L-glutamine, 1× penicillin–streptomycin and 50 ng/ml NGF2.5S (Millipore), and were incubated for 5–7 days. Primary RGCs were isolated from rat pups at postnatal day 4, as previously described (Barres et al., 1988). Purified RGCs were plated onto laminin- and poly-D-lysine-coated coverslips, and cultured in differentiation medium, comprising Neurobasal-A medium (Life Technologies) supplemented with 1× B-27 (Life Technologies), 1× Sato medium, 5 µg/ml insulin (Sigma), 1 mM sodium pyruvate (ThermoFisher), 1× T3 (Sigma), 1× N-acetyl cysteine (Sigma), 0.5 mM L-glutamine and gentamicin (Life Technologies). Primary cortical neurons were isolated by trypsinization (Life Technologies) of E14.5-mouse cortices and plated onto poly-D-lysine-coated (Sigma) coverslips (Zeiss) in Neurobasal-A medium (Life Technologies) supplemented with 1× B-27 (Life Technologies), 1× Sato medium, 0.5 mM L-glutamine and gentamicin (Life Technologies). RGCs were prepared and cultured as previously described (Barres et al., 1988). All cells were maintained at 37°C under 5% CO_2. COS-1 and PC12 cells, and primary neurons were transfected with Lipofectamine 2000 (Invitrogen) and 3T3 cells with Trans-IT (Mirus), as per the manufacturer's instructions. Stable transfectants were selected over two weeks in media containing either 1 µg/ml puromycin (Sigma) or 400 µg/ml Geneticin (Life Technologies). For Sort1 knockdown, four functional short hairpins and one scrambled control were tested, and efficiency of Sort1 knockdown was determined by western blotting. In cortical neurons, shRNA-expressing neurons were identified through GFP expression, and Sort1 knockdown was confirmed through a lack of Sort1 staining (immunocytochemistry).

Cell fractionation

Five 15-cm culture dishes of CHO and CHO-sortilin cells were transiently transfected with an expression construct for murine Shh using Lipofectamine 2000 from Invitrogen. After 48 h, cells were harvested and resuspended in 3 ml of homogenization buffer containing 10 mM HEPES, pH 7.4, 1 mM EDTA and 0.25 mM sucrose plus protease inhibitor cocktail Cømplete from Roche. Thereafter, cells were fractionated by performing a discontinuous iodixanol density gradient protocol, as described previously (Chang et al., 2003), and fractions were blotted for organelle-specific markers, Sort1 and Shh.

Western blotting and co-immunoprecipitation

Cells were lysed in ice-cold RIPA buffer with protease inhibitors (Roche), and protein concentration was determined using a standard Bradford assay. Lysates were subjected to SDS-PAGE, and proteins were transferred on to Hybond-C Extra membranes (Millipore). Membranes were incubated overnight at 4°C with primary antibodies (Table S2), followed by incubation with horseradish peroxidase (HRP)-conjugated secondary antibodies (Millipore) and were developed with an enhanced chemiluminescence (ECL) detection kit (Millipore). Densitometry was performed on bands using the blot analyzer function in ImageJ. For co-immunoprecipitation, transfected cells were lysed in ice-cold buffer containing 10 mM HEPES-NaOH pH7.4, 100 mM NaCl, 1% NP-40, 10% glycerol, and protease inhibitors (Roche). Clarified lysates were pre-cleared with Protein-A beads (Invitrogen) and then incubated with primary antibodies (Table S2) or species-matched nonspecific IgG, then precipitated using fresh Protein-A beads. Protein complexes were eluted from beads using SDS loading buffer, and analyzed by performing SDS-PAGE.

Analysis of induced secretion and luciferase assays

PC12 cells cultured in differentiation-inducing conditions were transfected with ShhFL, and subsequently incubated for 5–7 days. Cells were washed

twice with pre-warmed basal medium [5.6 mM KCl, 145 mM NaCl, 2.2 mM $CaCl_2$, 0.5 mM $MgCl_2$, 5.6 mM glucose, 15 mM HEPES-KOH (pH 7.4) and 0.1 mg/ml BSA], and incubated for 60 min with basal medium or stimulating medium [56 mM KCl, 95 mM NaCl, 2.2 mM $CaCl_2$, 0.5 mM $MgCl_2$, 5.6 mM glucose, 15 mM HEPES-KOH (pH 7.4) and 0.1 mg/ml BSA] with 1 mg/ml heparin. Cell culture supernatants were centrifuged at 10,000 ***g*** to remove cellular debris, and were analyzed by performing an ELISA, as per the manufacturer's instructions (R&D Systems). For luciferase assays, 3T3 cells were transiently transfected with *Renilla*–Luciferase and Gli–luciferase along with the indicated plasmids, serum-starved for 24 h and incubated with recombinant Shh (R&D Systems) for 24 h. Luciferase and *Renilla* activity was then measured, as per manufacturer instructions (Promega).

Proximity ligation assay

COS1 cells (10,000) were plated on poly-D-lysine+laminin-coated 16-well chamber slides (Nunc, Sigma) for 24 h. A serial dilution of plasmid concentrations (50, 100, 250, 500 and 1000 ng) was co-transfected (SortFL+Shh; BDNF–HA+Shh; and Fzd4–Myc) using Lipofectamine 3000 as per the manufacturer's instructions (ThermoFisher). Co-transfection with pMAX-GFP in preliminary studies was used as a transfection control. Single-plasmid transfections, no primary antibody and no plus-probe conditions were used as negative controls for PLA product synthesis. Cells were briefly washed in PBS and fixed for 10 min in 4% paraformaldehyde (Electron Microscopy Systems). Proximity ligation was performed as per manufacturer's instructions (Duolink Proximity Ligation Assay kit; Sigma). Optimal combinations of plasmid (100 ng per plasmid per well) and antibody (mouse anti-5E1, Developmental Studies Hybridoma Bank, 1:20,000; rabbit anti-sortilin, Abcam ab16640, 1:5000; rabbit anti-HA, Santa Cruz, Y-11, 1:5000; mouse anti-Myc, Sigma, PLA0001, 1:20,000) dilutions were determined in preliminary experiments. Co-transfection with the CellLight® Golgi-GFP, BacMam 2.0 (ThermoFisher) reporter (5 µl per well) was used as a trans-Golgi counterstain. Images (2048×2048) were acquired on a Zeiss LSM780 confocal microscope using a 40× water immersion objective. Pinhole diameter was set to 1.0 AU, and all laser and detector settings maintained across experimental groups. *z*-stacks were converted to 8-bit grayscale and imported into Blobfinder (Centre for Image Analysis, Uppsala University). Thresholding parameters used were as follows: minimum nucleus size in pixels squared=2800; cytoplasm size (radius)=100 pixels; blob size=3×3; blob threshold=50. Following Levene's test for homogeneity of variance tests, data were analyzed using a one-way ANOVA and Scheffé's post hoc tests in SPSS 21 software.

Mouse lines and *in utero* electroporation

Animal husbandry was performed in accordance with the Association for Research in Vision and Ophthalmology (ARVO) Statement for the Use of Animals in Ophthalmic and Vision Research, and the University of Ottawa Animal Care Committee. Wild-type CD1 mice (Charles River) were used for the isolation of primary cortical neurons. Sort1-mutant ($Sort1^{-/-}$) mice (genotyped by performing PCR using the following primers: F - 5′-CTC-AGGAATGGCATTCTCAG-3′, R - 5′-AGCCTTTACCTGGTGTCATC-3′) (Zeng et al., 2009) and Shh::GFP mice (Jackson Labs) [genotyped as described previously (Chamberlain et al., 2008)] were maintained on a C57/Bl6J background (Charles River). F2 mice from $Sort1^{+/-}\times Shh^{+/GFP}$ matings were mated to generate Sort1;Shh::GFP double mutants and littermate controls at E11.5 and E14.5. Mice were mated in the afternoon, and the presence of a vaginal plug the next morning was considered E0.5. *In utero* electroporation was performed as previously described (Garcia-Frigola et al., 2007) at E13.5, and cells in S-phase were labelled *in vivo* through an intra-peritoneal injection of the dam with EdU (Life Technologies) 1 h before mice were killed at E15.5.

Immunocytochemistry, immunohistochemistry, *in situ* hybridization and hematoxylin and eosin staining

Cells cultured on poly-D-lysine-coated coverslips were fixed in 4% PFA for 5–20 min and permeabilized with 0.1% Triton-X100 (as indicated). Fixed cells were incubated overnight at 4°C with primary antibodies (Table S2), followed by incubation with fluorophore-conjugated secondary antibodies (1:1000, Life Technologies). Nuclei were stained with Hoechst 33342 (1:25,000; Invitrogen). Coverslips were mounted on permafrost slides (Fisher) with fluorescent mounting medium (Dako). Embryonic tissue was fixed overnight in 4% PFA, cryoprotected in sucrose and frozen in 50:50 30% sucrose:OCT. *In situ* hybridization was performed on frozen sections using a digoxigenin-labeled antisense probe against *Vsx2*. For immunohistochemistry, frozen sections were stained with rabbit anti-GFP and goat anti-Pax2 (1:200; Covance) antibodies (Table S2), and nuclei were stained with Hoechst 3342, and EdU was detected using the 543-nm fluorophore click-IT reaction kit (Life Technologies). For hematoxylin and eosin staining, frozen sections were rehydrated with PBS, stained with hematoxylin, washed and dehydrated using an ethanol series, stained with eosin and rehydrated before mounting.

Microscopy and image analysis

Immunohistochemistry and immunocytochemistry samples were imaged using a Zeiss LSM510 META confocal microscope with 63×1.4 oil Plan-Appochromat or 20×0.5 EC Plan-Neofluar objectives and the Zen 2009 software; or a Zeiss Axio Imager M2 instrument with 63×1.4 oil Plan-Apochromat or 20×0.8 Ph2 Plan-Apochromat objectives and AxioVision Rel. 4.8 software. Only cells with an intact nucleus and low-to-medium expression of transfected constructs were imaged. In neuron images, axons were identified by length (the longest process was at least ten times the diameter of the neuron body in length), protrusion of few branches and by positive staining for Tau. For distribution analysis, 1-µm optical sections of individual neurons were imaged using a constant gain, and the pixel intensity was measured using ImageJ, with the mean ratio of signal in the axon compared to the soma calculated from measurements of the indicated number of neurons. Colocalization with organelle markers was quantified in 1-µm sections of individual neurons using the Intensity Correlation Analysis plug-in in ImageJ, and mean Pearson's correlation coefficients were compared between conditions.

Acknowledgements

We thank Dr Francis Lee for the BDNF–HA construct, and Dr Peter Madsen for sortilin constructs. We would also like to thank Sherry Thurig, Katy Morin and Sheila Smiley for performing animal husbandry; Melanie Liekweg and Christine Kruse for expert technical assistance; and Dr Alan Mears for work on sortilin genotyping. Finally, we thank Drs Carlos Morales and Dr Frederic Charron for their insightful comments and suggestions.

Competing interests

The authors declare no competing or financial interests.

Author contributions

C.C., experimental conception, design, data acquisition, analysis, interpretation, manuscript preparation, revision. S.B., experimental conception, design, data acquisition, interpretation, manuscript revision. P.E.B.N., data acquisition, interpretation, manuscript preparation. J.P., experimental conception, design, data acquisition, manuscript revision. C.M., data acquisition, analysis. E.A.B., data interpretation, manuscript preparation. R.R., experimental conception, design, data interpretation. F.A.J., data acquisition, interpretation. C.M., data interpretation, manuscript revision. A.C., data interpretation, manuscript revision. V.A.W., experimental conception, design, data analysis, interpretation, manuscript preparation, revision.

Funding

This work was supported by an operating grant [number 97765] from the Canadian Institutes of Health Research to V.A.W.; and a postdoctoral fellowship from Helmholtz-Gemeinschaft to A.C.

Supplementary information

Supplementary information available online at
http://jcs.biologists.org/lookup/doi/10.1242/jcs.183541.supplemental

References

Aikin, R., Cervantes, A., D'Angelo, G., Ruel, L., Lacas-Gervais, S., Schaub, S. and Thérond, P. (2012). A genome-wide RNAi screen identifies regulators of cholesterol-modified hedgehog secretion in Drosophila. *PLoS ONE* **7**, e33665.

Barres, B. A. and Raff, M. C. (1993). Proliferation of oligodendrocyte precursor cells depends on electrical activity in axons. *Nature* **361**, 258-260.

Barres, B. A., Silverstein, B. E., Corey, D. P. and Chun, L. L. Y. (1988). Immunological, morphological, and electrophysiological variation among retinal ganglion cells purified by panning. *Neuron* **1**, 791-803.
Barres, B. A., Jacobson, M. D., Schmid, R., Sendtner, M. and Raff, M. C. (1993). Does oligodendrocyte survival depend on axons? *Curr. Biol.* **3**, 489-497.
Beug, S. T., Parks, R. J., McBride, H. M. and Wallace, V. A. (2011). Processing-dependent trafficking of Sonic hedgehog to the regulated secretory pathway in neurons. *Mol. Cell. Neurosci.* **46**, 583-596.
Briscoe, J. and Thérond, P. P. (2013). The mechanisms of Hedgehog signalling and its roles in development and disease. *Nat. Rev. Mol. Cell Biol.* **14**, 416-429.
Burne, J. F. and Raff, M. (1997). Retinal ganglion cell axons drive the proliferation of astrocytes in the developing rodent optic nerve. *Neuron* **18**, 223-230.
Callejo, A., Bilioni, A., Mollica, E., Gorfinkiel, N., Andrés, G., Ibáñez, C., Torroja, C., Doglio, L., Sierra, J. and Guerrero, I. (2011). Dispatched mediates Hedgehog basolateral release to form the long-range morphogenetic gradient in the Drosophila wing disk epithelium. *Proc. Natl. Acad. Sci. USA* **108**, 12591-12598.
Canuel, M., Korkidakis, A., Konnyu, K. and Morales, C. R. (2008). Sortilin mediates the lysosomal targeting of cathepsins D and H. *Biochem. Biophys. Res. Commun.* **373**, 292-297.
Capurro, M. I., Shi, W. and Filmus, J. (2012). LRP1 mediates Hedgehog-induced endocytosis of the GPC3-Hedgehog complex. *J. Cell Sci.* **125**, 3380-3389.
Chamberlain, C. E., Jeong, J., Guo, C., Allen, B. L. and McMahon, A. P. (2008). Notochord-derived Shh concentrates in close association with the apically positioned basal body in neural target cells and forms a dynamic gradient during neural patterning. *Development* **135**, 1097-1106.
Chang, Y., Tesco, G., Jeong, W. J., Lindsley, L., Eckman, E. A., Eckman, C. B., Tanzi, R. E. and Guenette, S. Y. (2003). Generation of the beta-amyloid peptide and the amyloid precursor protein C-terminal fragment gamma are potentiated by FE65L1. *J. Biol. Chem.* **278**, 51100-51107.
Chen, Z.-Y., Ieraci, A., Teng, H., Dall, H., Meng, C.-X., Herrera, D. G., Nykjaer, A., Hempstead, B. L. and Lee, F. S. (2005). Sortilin controls intracellular sorting of brain-derived neurotrophic factor to the regulated secretory pathway. *J. Neurosci.* **25**, 6156-6166.
Chen, X., Tukachinsky, H., Huang, C.-H., Jao, C., Chu, Y.-R., Tang, H.-Y., Mueller, B., Schulman, S., Rapoport, T. A. and Salic, A. (2011). Processing and turnover of the Hedgehog protein in the endoplasmic reticulum. *J. Cell Biol.* **192**, 825-838.
Chiang, C., Litingtung, Y., Lee, E., Young, K. E., Corden, J. L., Westphal, H. and Beachy, P. A. (1996). Cyclopia and defective axial patterning in mice lacking Sonic hedgehog gene function. *Nature* **383**, 407-413.
Dakubo, G. D., Wang, Y. P., Mazerolle, C., Campsall, K., McMahon, A. P. and Wallace, V. A. (2003). Retinal ganglion cell-derived sonic hedgehog signaling is required for optic disc and stalk neuroepithelial cell development. *Development* **130**, 2967-2980.
Dakubo, G. D., Beug, S. T., Mazerolle, C. J., Thurig, S., Wang, Y. and Wallace, V. A. (2008). Control of glial precursor cell development in the mouse optic nerve by sonic hedgehog from retinal ganglion cells. *Brain Res.* **1228**, 27-42.
D'Angelo, G., Matusek, T., Pizette, S. and Thérond, P. P. (2015). Endocytosis of Hedgehog through dispatched regulates long-range signaling. *Dev. Cell* **32**, 290-303.
Evans, S. F., Irmady, K., Ostrow, K., Kim, T., Nykjaer, A., Saftig, P., Blobel, C. and Hempstead, B. L. (2011). Neuronal brain-derived neurotrophic factor is synthesized in excess, with levels regulated by sortilin-mediated trafficking and lysosomal degradation. *J. Biol. Chem.* **286**, 29556-29567.
Garcia-Frigola, C., Carreres, M., Vegar, C. and Herrera, E. (2007). Gene delivery into mouse retinal ganglion cells by in utero electroporation. *BMC Dev. Biol.* **7**, 103.
Goodrich, L., Milenković, L., Higgins, K. M. and Scott, M. P. (1997). Altered neural cell fates and medulloblastoma in mouse patched mutants. *Science* **277**, 1109-1113.
Gradilla, A. C., González, E., Seijo, I., Andrés, G., Bischoff, M., González-Mendez, L., Sánchez, V., Callejo, A., Ibáñez, C., Guerra, M. et al. (2014). Exosomes as Hedgehog carriers in cytoneme-mediated transport and secretion. *Nat. Commun.* **5**, 5649.
Greene, L. A. and Tischler, A. S. (1976). Establishment of a noradrenergic clonal line of rat adrenal pheochromocytoma cells which respond to nerve growth factor. *Proc. Natl. Acad. Sci. USA* **73**, 2424-2428.
Guerrero, I. and Kornberg, T. B. (2014). Hedgehog and its circuitous journey from producing to target cells. *Semin. Cell Dev. Biol.* **33**, 52-62.
Hampe, W., Riedel, I., Lintzel, J., Bader, C., Franke, I. and Schaller, H. (2000). Ectodomain shedding, translocation and synthesis of SorLA are stimulated by its ligand head activator. *J. Cell Sci.* **113**, 4475-4485.
Hassan, A. J., Zeng, J., Ni, X. and Morales, C. R. (2004). The trafficking of prosaposin (SGP-1) and GM2AP to the lysosomes of TM4 Sertoli cells is mediated by sortilin and monomeric adaptor proteins. *Mol. Reprod. Dev.* **68**, 476-483.
Hermans-Borgmeyer, I., Hermey, G., Nykjaer, A. and Chica Schaller, A. (1999). Expression of the 100-kDa neurotensin receptor sortilin during mouse embryonal development. *Mol. Brain Res.* **65**, 216-219.
Hermey, G., Keat, S. J., Madsen, P., Jacobsen, C., Petersen, C. M. and Gliemann, J. (2003). Characterization of sorCS1, an alternatively spliced receptor with completely different cytoplasmic domains that mediate different trafficking in cells. *J. Biol. Chem.* **278**, 7390-7396.
Huang, Z. and Kunes, S. (1996). Hedgehog, transmitted along retinal axons, triggers neurogenesis in the developing visual centers of the Drosophila brain. *Cell* **86**, 411-422.
Huang, C.-H., Hsiao, C.-H., Chu, Y.-R., Ye, Y. and Chen, X. (2013). Derlin2 protein facilitates HRD1-mediated retro-translocation of sonic hedgehog at the endoplasmic reticulum. *J. Biol. Chem.* **288**, 25330-25339.
Jacobsen, L., Madsen, P., Moestrup, S. K., Lund, A. H., Tommerup, N., Nykjaer, A., Sottrup-Jensen, L., Gliemann, J. and Petersen, C. M. (1996). Molecular characterization of a novel human hybrid-type receptor that binds the alpha2-macroglobulin receptor-associated protein. *J. Biol. Chem.* **271**, 31379-31383.
Jansen, P., Giehl, K., Nyengaard, J. R., Teng, K., Lioubinski, O., Sjoegaard, S. S., Breiderhoff, R., Gotthardt, M., Lin, F., Ellers, A. et al. (2007). Roles for the pro-neurotrophin receptor sortilin in neuronal development, aging and brain injury. *Nat. Neurosci.* **10**, 1449-1457.
Jiang, J. and Hui, C.-c. (2008). Hedgehog signaling in development and cancer. *Dev. Cell* **15**, 801-812.
Karpen, H. E., Bukowski, J. T., Hughes, T., Gratton, J.-P., Sessa, W. C. and Gailani, M. R. (2001). The sonic hedgehog receptor patched associates with caveolin-1 in cholesterol-rich microdomains of the plasma membrane. *J. Biol. Chem.* **276**, 19503-19511.
Kocks, C., Maehr, R., Overkleeft, H. S., Wang, E. W., Iyer, L. K., Lennon-Dumenil, A.-M., Ploegh, H. L.and Kessler, B. M. (2003). Functional proteomics of the active cysteine protease content in Drosophila S2 cells. *Mol. Cell. Proteomics* **2**, 1188-1197.
Lebrun-Julien, F., Bertrand, M. J., De Backer, O., Stellwagen, D., Morales, C. R., Di Polo, A. and Barker, P. A. (2010). ProNGF induces TNFalpha-dependent death of retinal ganglion cells through a p75NTR non-cell-autonomous signaling pathway. *Proc. Natl. Acad. Sci. USA* **107**, 3817-3822.
Lee, J., Ekker, S., von Kessler, D., Porter, J., Sun, B. and Beachy, P. (1994). Autoproteolysis in hedgehog protein biogenesis. *Science* **226**, 1528-1537.
Lefrancois, S., Zeng, J., Hassan, A., Canuel, M. and Morales, C. R. (2003). The lysosomal trafficking of sphingolipid activator proteins (SAPs) is mediated by sortilin. *EMBO J.* **22**, 6430-6437.
Li, F., Shi, W., Capurro, M. and Filmus, J. (2011). Glypican-5 stimulates rhabdomyosarcoma cell proliferation by activating Hedgehog signaling. *J. Cell Biol.* **192**, 691-704.
Litingtung, Y. and Chiang, C. (2000). Specification of ventral neuron types is mediated by an antagonistic interaction between Shh and Gli3. *Nat. Neurosci.* **3**, 979-985.
Maity, T., Fuse, N. and Beachy, P. A. (2005). Molecular mechanisms of Sonic hedgehog mutant effects in holoprosencephaly. *Proc. Natl. Acad. Sci. USA* **102**, 17026-17031.
Marcusson, E. G., Horazdovsky, B. F., Cereghino, J. L., Gharakhanian, E. and Emr, S. D. (1994). The sorting receptor for yeast vacuolar carboxypeptidase Y is encoded by the VPS10 gene. *Cell* **77**, 579-586.
Matusek, T., Wendler, F., Polès, S., Pizette, S., D'Angelo, G., Fürthauer, M. and Thérond, P. P. (2014). The ESCRT machinery regulates the secretion and long-range activity of Hedgehog. *Nature* **516**, 99-103.
Munck Petersen, C., Nielsen, M. S., Jacobsen, C., Tauris, J., Jacobsen, L., Gliemann, J., Moestrup, S. K. and Madsen, P. (1999). Propeptide cleavage conditions sortilin/neurotensin receptor-3 for ligand binding. *EMBO J.* **18**, 595-604.
Nakamura, K., Namekata, K., Harada, C. and Harada, T. (2007). Intracellular sortilin expression pattern regulates proNGF-induced naturally occurring cell death during development. *Cell Death Differ.* **14**, 1552-1554.
Ni, X. and Morales, C. R. (2006). The lysosomal trafficking of acid sphingomyelinase is mediated by sortilin and mannose 6-phosphate receptor. *Traffic* **7**, 889-902.
Nielsen, M. S., Madsen, P., Christensen, E. I., Nykjaer, A., Gliemann, J., Kasper, D., Pohlmann, R. and Petersen, C. M. (2001). The sortilin cytoplasmic tail conveys Golgi-endosome transport and binds the VHS domain of the GGA2 sorting protein. *EMBO J.* **20**, 2180-2190.
Nykjaer, A., Lee, R., Teng, K. K., Jansen, P., Madsen, P., Nielsen, M. S., Jacobsen, C., Kliemannel, M., Schwarz, E., Willnow, T. E. et al. (2004). Sortilin is essential for proNGF-induced neuronal cell death. *Nature* **427**, 843-848.
Parchure, A., Vyas, N., Ferguson, C., Parton, R. G. and Mayor, S. (2015). Oligomerization and endocytosis of Hedgehog is necessary for its efficient exovesicular secretion. *Mol. Biol. Cell* **26**, 4700-4717.
Pepinsky, R. B., Zeng, C., Wen, D., Rayhorn, P., Baker, D. P., Williams, K. P., Bixler, S. A., Ambrose, C. M., Garber, E. A., Miatkowski, K. et al. (1998). Identification of a palmitic acid-modified form of human Sonic hedgehog. *J. Biol. Chem.* **273**, 14037-14045.
Petersen, C. M., Nielsen, M. S., Nykjaer, A., Jacobsen, L., Tommerup, N., Rasmussen, H. H., Roigaard, H., Gliemann, J., Madsen, P. and Moestrup, S. K. (1997). Molecular identification of a novel candidate sorting receptor purified

from human brain by receptor-associated protein affinity chromatography. *J. Biol. Chem.* **272**, 3599-3605.

Petralia, R., Wang, Y.-X., Mattson, M. P. and Yao, P. J. (2011). Sonic hedgehog distribution within mature hippocampal neurons. *Commun. Integr. Biol.* **4**, 775-777.

Porter, J. A., von Kessler, D. P., Ekker, S. C., Young, K. E., Lee, J. J., Moses, K. and Beachy, P. A. (1995). The product of hedgehog autoproteolytic cleavage active in local and long-range signalling. *Nature* **374**, 363-366.

Porter, J. A., Young, K. E. and Beachy, P. A. (1996). Cholesterol modification of hedgehog signaling proteins in animal development. *Science* **274**, 255-259.

Rezgaoui, M., Hermey, G., Riedel, I., Hampe, W., Schaller, H. and Hermans-Borgmeyer, I. (2001). Identification of SorCS2, a novel member of the VPS10 domain containing receptor family, prominently expressed in the developing mouse brain. *Mech. Dev.* **100**, 335-338.

Roessler, E., Belloni, E., Gaudenz, K., Jay, P., Berta, P., Scherer, S., Tsui, L.-C. and Muenke, M. (1996). Mutations in the human Sonic Hedgehog gene cause holoprosencephaly. *Nat. Genet.* **14**, 357-360.

Schell-Apacik, C., Rivero, M., Knepper, J. L., Roessler, E., Muenke, M. and Ming, J. E. (2003). SONIC HEDGEHOG mutations causing human holoprosencephaly impair neural patterning activity. *Hum. Genet.* **113**, 170-177.

Shevchenko, A., Schaft, D., Roguev, A., Pijnappel, W. W. M. P., Stewart, A. F. and Shevchenko, A. (2002). Deciphering protein complexes and protein interaction networks by tandem affinity purification and mass spectrometry: analytical perspective. *Mol. Cell. Proteomics* **1**, 204-212.

Söderberg, O., Gullberg, M., Jarvius, M., Ridderstråle, K., Leuchowius, K.-J., Jarvius, J., Wester, K., Hydbring, P., Bahram, F., Larsson, L.-G. et al. (2006). Direct observation of individual endogenous protein complexes in situ by proximity ligation. *Nat. Methods* **3**, 995-1000.

Söderberg, O., Leuchowius, K.-J., Gullberg, M., Jarvius, M., Weibrecht, I., Larsson, L.-G. and Landegren, U. (2008). Characterizing proteins and their interactions in cells and tissues using the in situ proximity ligation assay. *Methods* **45**, 227-232.

Soukkarieh, C., Agius, E., Soula, C. and Cochard, P. (2007). Pax2 regulates neuronal–glial cell fate choice in the embryonic optic nerve. *Dev. Biol.* **303**, 800-813.

Tao, C. and Zhang, X. (2014). Development of astrocytes in the vertebrate eye. *Dev. Dyn.* **243**, 1501-1510.

Teng, H. K., Teng, K. K., Lee, R., Wright, S., Tevar, S., Almeida, R. D., Kermani, P., Torkin, R., Chen, Z.-Y., Lee, F. S. et al. (2005). ProBDNF induces neuronal apoptosis via activation of a receptor complex of p75NTR and sortilin. *J. Neurosci.* **25**, 5455-5463.

Tokhunts, R., Singh, S., Chu, T., D'Angelo, G., Baubet, V., Goetz, J. A., Huang, Z., Yuan, A., Ascano, M. Zavros, Y. et al. (2010). The full-length unprocessed hedgehog protein is an active signaling molecule. *J. Biol. Chem.* **285**, 2562-2568.

Trinkle-Mulcahy, L., Boulon, S., Lam, Y. W., Urcia, R., Boisvert, F.-M., Vandermoere, F., Morrice, N. A., Swift, S., Rothbauer, U., Leonhardt, H. et al. (2008). Identifying specific protein interaction partners using quantitative mass spectrometry and bead proteomes. *J. Cell Biol.* **183**, 223-239.

Vaegter, C. B., Jansen, P., Fjorback, A. W., Glerup, S., Skeldal, S., Kjolby, M., Richner, M., Erdmann, B., Nyengaard, J. R., Tessarollo, L. et al. (2011). Sortilin associates with Trk receptors to enhance anterograde transport and neurotrophin signaling. *Nat. Neurosci.* **14**, 54-61.

Vyas, N., Walvekar, A., Tate, D., Lakshmanan, V., Bansal, D., Lo Cicero, A., Raposo, G., Palakodeti, D. and Dhawan, J. (2014). Vertebrate Hedgehog is secreted on two types of extracellular vesicles with different signaling properties. *Sci. Rep.* **4**, 7357.

Wallace, V. A. and Raff, M. (1999). A role for Sonic hedgehog in axon-to-astrocyte signaling in the rodent optic nerve. *Development* **126**, 2901-2909.

Wang, Y., Dakubo, G. D., Thurig, S., Mazerolle, C. J. and Wallace, V. A. (2005). Retinal ganglion cell-derived sonic hedgehog locally controls proliferation and the timing of RGC development in the embryonic mouse retina. *Development* **132**, 5103-5113.

Yang, M., Lim, Y., Li, X., Zhong, J.-H. and Zhou, X.-F. (2011). Precursor of brain-derived neurotrophic factor (proBDNF) forms a complex with Huntingtin-associated protein-1 (HAP1) and sortilin that modulates proBDNF trafficking, degradation, and processing. *J. Biol. Chem.* **286**, 16272-16284.

Yang, M., Virassamy, B., Vijayaraj, S. L. Lim, Y., Saadipour, K., Wang, Y.-J., Han, Y.-C., Zhong, J.-H., Morales, C. R. and Zhou, X.-F. (2013). The intracellular domain of sortilin interacts with amyloid precursor protein and regulates its lysosomal and lipid raft trafficking. *PLoS ONE* **8**, e63049.

Zeng, J., Racicott, J. and Morales, C. R. (2009). The inactivation of the sortilin gene leads to a partial disruption of prosaposin trafficking to the lysosomes. *Exp. Cell Res.* **315**, 3112-3124.

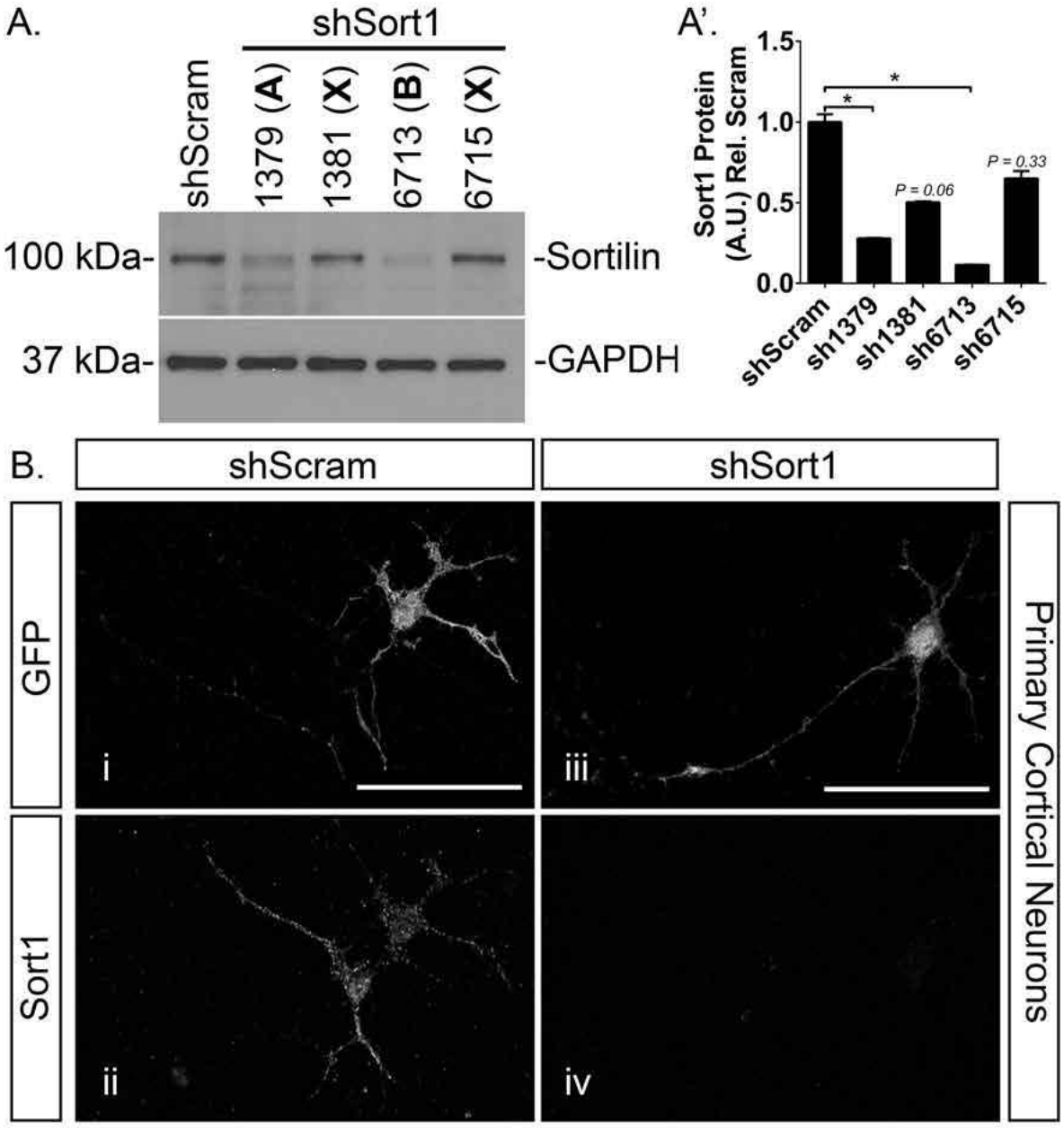
A.
shScram
shSort1
1379 (A)
1381 (X)
6713 (B)
6715 (X)
100 kDa-
-Sortilin
37 kDa-
-GAPDH
A'.
Sort1 Protein (A.U.) Rel. Scram
1.5
1.0
0.5
0.0
*
*
P = 0.06
P = 0.33
shScram
sh1379
sh1381
sh6713
sh6715
B.
shScram
shSort1
GFP
Sort1
i
ii
iii
iv
Primary Cortical Neurons

Supplemental Figure 1: Validation of short hairpin-mediated Sortilin knockdown. (A, A') Representative western blots analysis of Sort1 levels in 3T3 cells transiently transfected with a control short hairpin (shScram), or the indicated shSort1 constructs. GAPDH is used as a loading control. Functional short hairpin chosen for further analysis are indicated as "A" and "B", and indicated as shSort1 A or B subsequently in the text. (A') Sort1 protein densitometry was performed on blots in A using the Gels function on ImageJ. Bars indicate mean Sort1 levels from three independent experiments, normalized to GAPDH, relative to scrambled control. Error bars represent S.E.M., * $P < 0.05$, Student's t-test. **(B)** Expression of functional Sort1 KD constructs correlates with a reduction of Sort1 signal in primary neurons. ICC on fixed and permeabilized CNs. GFP indicates transfected cells and (i, iii), Sort1 KD confirmed by staining with α-Sort1 antibody (ii, iv). Scale bars, 10μm.

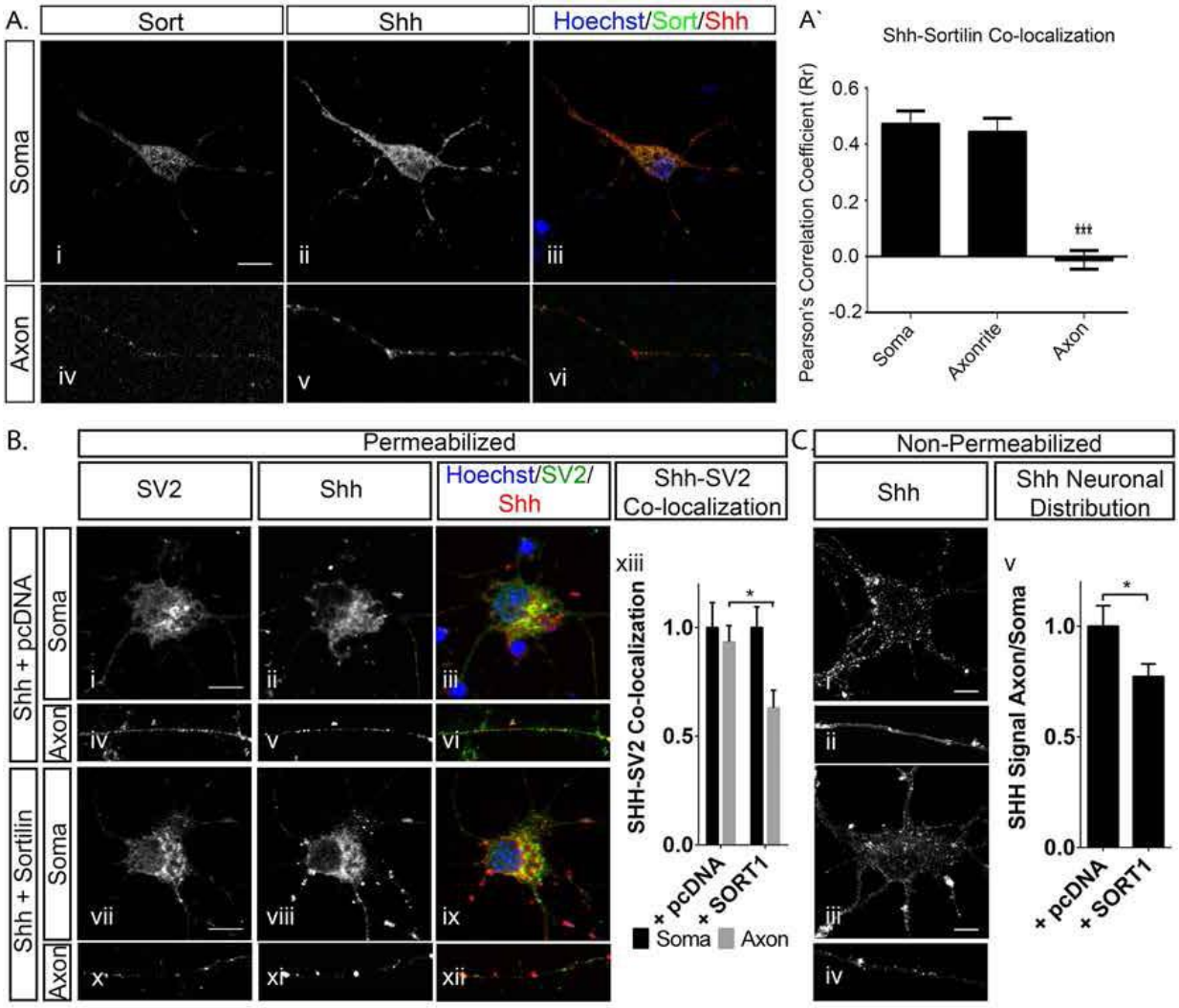

Supplemental Figure 2: Overexpressed Shh and endogenous Sort1 co-localize extensively in the somatodendritic compartment, but not in axons, in primary CNs. **(A)** ICC and Hoechst nuclear staining on fixed and permeabilized CNs. Panels show 1μm optic sections in the somatodendritic (upper), or axonal (lower) compartments. Scale bars, 10μm. **(A')** Quantification of the co-localization of Shh and Sort1 in the indicated subcellular compartment in CNs. Bars represent mean Pearson's Correlation Coeffecient (Rr) ($n > 5$ cells per condition). Error bars represent S.E.M., * $p < 0.05$, Student's t-test. **(B)** Overexpression of Sort reduces Shh trafficking to the axon in cortical neurons. Sort1 overexpression reduces the co-localization of Shh with SV2. Representative IHC on fixed and permeabilized primary CNs expressing Shh and pcDNA (i-vi) or Sort1 (vii-xii). Panels show 1μm optic sections in the somatodendritic (upper), or axonal (lower) compartments. Scale bars, 10μm. Co-localization of Shh and SV2 was quantified using

the Intensity Correlation Analysis function in ImageJ (xiii). Bars indicate mean Pearson's Correlation Coeffecient (Rr) (n = 20 neurons per condition) normalized to control conditions. Error bars represent S.E.M., * $p < 0.05$, Student's t-test. **(C)** Sort1 overexpression correlates with a reduction in the ratio of Shh signal on the surface of the axon relative to the soma. Representative ICC on fixed, non-permeabilized primary CNs expressing Shh and shScram (i-ii) or shSort1 (iii-iv). Panels show 1μm optic sections in the somatodendritic (upper), or axonal (lower) panels. Scale bars, 10μm. Shh distribution quantified as the ratio of Shh signal intensity in a distal region of the axon relative to signal intensity in the soma (v). Bars represent mean ratio of axon: soma Shh signal (n = 20 neurons per condition) normalized to control conditions. Error bars represent S.E.M., * $p < 0.05$, Student's t-test.

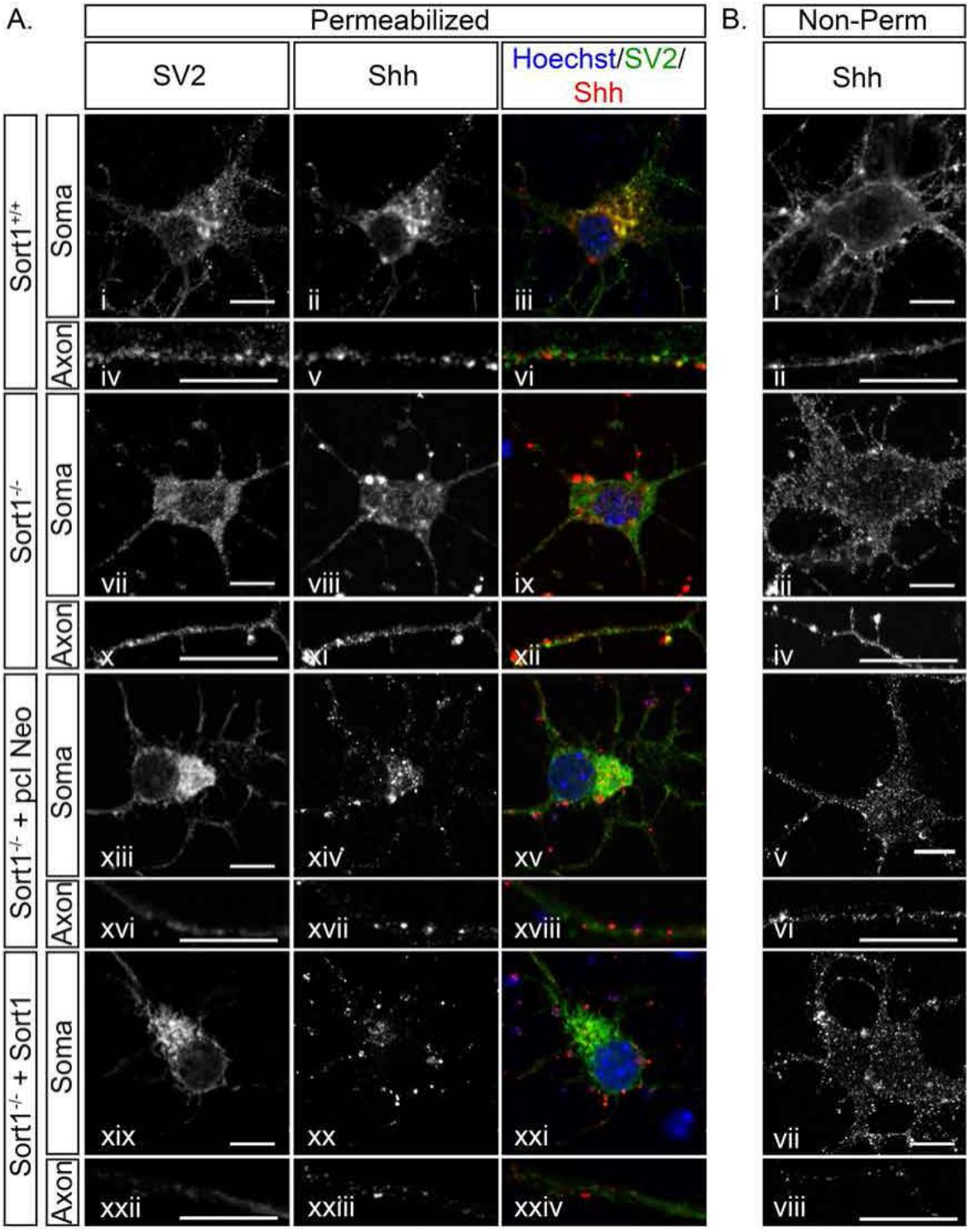

Supplemental Figure 3: Sort1 expression negatively correlates with distribution of Shh in axons. (A) Sort1$^{-/-}$ increased the colocalization of Shh with SV2, Sort1 overexpression in Sort1$^{-/-}$ rescued the phenotype. ICC and Hoechst nuclear staining on fixed and permeabilized primary cortical neurons expressing Shh in Sort1$^{-/-}$ mice (i - xii), or from Sort1$^{-/-}$ mice overexpressing Sort1 (xiii - xxiv). Panels show 1μm optic sections in the somatodendritic (upper), or axonal (lower) compartments. Scale bars, 10μm. Co-localization quantified in Fig 4Di, Ei. **(B)** Sort1$^{-/-}$ correlates with increased ratio of Shh signal on the surface of the axon relative to the soma, Sort1 overexpression in Sort1$^{-/-}$ rescued the phenotype. Sort1 KD correlates with increased ratio of Shh signal on the surface of the axon relative to the soma. ICC on fixed, non-permeabilized primary cortical neurons expressing Shh in Sort1$^{-/-}$ mice (i - iv), or from Sort1$^{-/-}$ mice overexpressing Sort1 (v - viii). Panels show 1μm optic sections in the somatodendritic (upper), or axonal (lower) panels. Scale bars, 10μm. Shh distribution quantified in Fig 4Dii, Eii.

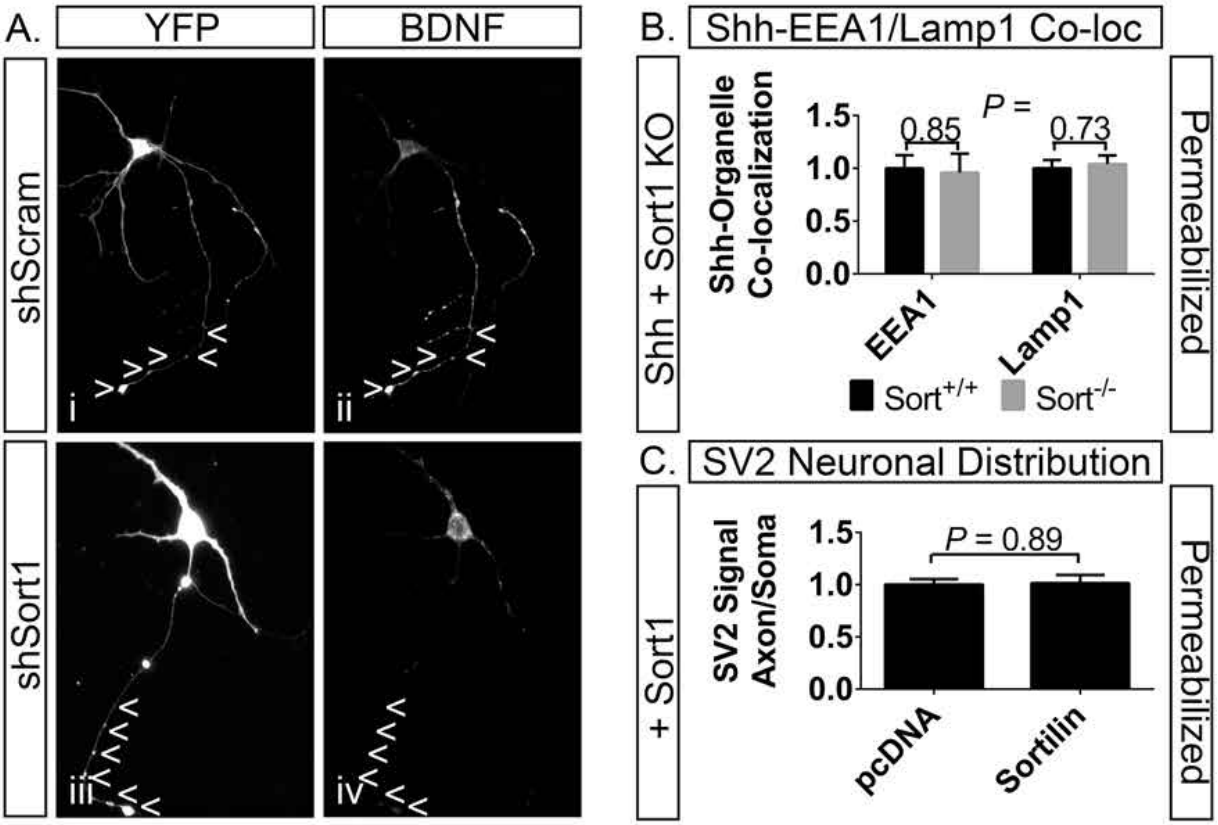

Supplemental Figure 4: Sort1 perturbation reduces BDNF-HA targeting to the axon, does not affect Shh endosomal or lysosomal targeting, and does not impair SV2+ vesicle biogenesis. **(A)** Sort1 KD reduced BDNF targeting to axons. ICC on fixed, permeabilized primary cortical neurons transiently transfected with BDNF-HA and shScram (top panels) or shSort1 (bottom panels). Panels show GFP (expressed through an IRES on the sh constructs) and BDNF-HA. ">" denotes axonal compartments, as determined by morphology and YFP staining, Scale bars, 10um. **(B)** Sort1 expression does not correlate with changes in Shh co-localization with EEA1 or Lamp1 + vesicles. Co-localization of Shh and EEA1 or Lamp1 in $Sort1^{+/+}$ and $Sort1^{-/-}$ CNs, quantified using the Intensity Correlation Analysis function in ImageJ. Bars indicate mean Pearson's Correlation Coeffecient (Rr) (n = 20 neurons per condition) normalized to control conditions. Error bars represent S.E.M., * $p < 0.05$, Student's t-test. **(C)** Sort1 overexpression does not correlate with a change in the ratio of SV2 signal in the axon relative to the soma. SV2 neuronal distribution quantified as the ratio of SV2 signal intensity in a distal region of the axon relative to signal intensity in the soma in CNs expressing pcDNA or Sort1-myc his. Bars indicate mean ratio of axon:soma SV2 signal (n = 20 neurons per condition) normalized to control conditions. Error bars represent S.E.M., * $p < 0.05$, Student's t-test.

Supplemental Table 1: Novel Shh interacting candidates identified in a Shh GST affinity screen. Interacting candidates identified using a GST affinity screen using ShhN-GST or ShhC-GST as bait, and rat brain microsomal fraction as prey. Candidates were prioritized based on peptide abundance and MASCOT score, with common Sepharose bead artifacts and cytoplasmic localized proteins excluded. Sheet 1 indicates ShhN interactors, Sheet 2 indicates ShhC interactors. Candidates are grouped according to the detergent used to generate the microsomal fraction, either NP40 (top) or CHAPS (bottom), and are represented by name and relevant accession number.

Bait	Detergent	Interacting Protein	Accession Number
ShhN	NP40	Agrin	gi|202799
ShhN	NP40	Neurexin II	gi|205715
ShhN	NP40	Kif1a	gi|109487519
ShhN	NP40	myotonic dystrophy kinase-related Cdc42-binding kinase MRCK-beta [Rattus norvegicus]	gi|2736153
ShhN	NP40	triple functional domain (PTPRF interacting)	gi|109464537
ShhN	NP40	Development and differentiation-enhancing factor 2	gi|109478077
ShhN	NP40	SSTR4	gi|7514122
ShhN	CHAPS	low density lipoprotein receptor-related protein	gi|62652278
ShhN	CHAPS	Agrin	gi|202799
ShhN	CHAPS	glypican 5	gi|109501994
ShhN	CHAPS	podocalyxin-like 2	gi|109472343
ShhN	CHAPS	FASN	gi|55775
ShhN	CHAPS	PI-3-kinase-related kinase SMG-1	gi|109462744
ShhN	CHAPS	Neurexin 1/2	gi|124106289
ShhN	CHAPS	chondroitin sulfate proteoglycan NG2	gi|539947
ShhN	CHAPS	chondroitin sulfate proteoglycan 5	gi|41281651
ShhN	CHAPS	Dmx-like 2	gi|109483500
ShhN	CHAPS	neuroglycan C	gi|1585922
ShhN	CHAPS	FAT tumor suppressor homolog 4	gi|109464786
ShhN	CHAPS	Kif1a	gi|109487519
ShhN	CHAPS	Kif1b	gi|52313412
ShhN	CHAPS	Cdc42-binding protein kinase beta	gi|76257394
ShhN	CHAPS	Plexin	gi|109481881
ShhN	CHAPS	neural cell adhesion molecule	gi|13928706
ShhN	CHAPS	roundabout homolog 1	gi|11559953
ShhN	CHAPS	triple functional domain (PTPRF interacting)	gi|109464537
ShhN	CHAPS	rapamycin and FKBP12 target-1 protein	gi|9845251
ShhN	CHAPS	acetyl-coenzyme A carboxylase alpha	gi|11559962
ShhN	CHAPS	similar to CG5937-PA	gi|109457596
ShhN	CHAPS	odd Oz/ten-m homolog	gi|109459066
ShhN	CHAPS	neurofibromatosis 1	gi|6981264
ShhN	CHAPS	FASN	gi|56621
ShhN	CHAPS	fat3 [Rattus norvegicus]	gi|19924085
ShhN	CHAPS	insulin-like growth factor 2 receptor	gi|6981078
ShhN	CHAPS	Sortilin-related receptor SorLA	gi|109484566
ShhN	CHAPS	neurestin alpha	gi|9910320
ShhN	CHAPS	neuropilin	gi|2407643
ShhC	NP40	sortilin 1	gi|109465375
ShhC	NP40	glycoprotein, synaptic 2	gi|19924091
ShhC	NP40	SSTR4	gi|7514122
ShhC	CHAPS	sortilin 1	gi|109465375
ShhC	CHAPS	glycoprotein, synaptic 2	gi|19924091
ShhC	CHAPS	collapsin response mediator proteins	gi|1518520
ShhC	CHAPS	ilvB (bacterial acetolactate synthase)-like	gi|34862359
ShhC	CHAPS	synaptotagmin P65 - rat	gi|92791
ShhC	CHAPS	synaptotagmin 2 [Rattus norvegicus]	gi|6981624
ShhC	CHAPS	copine 7/4	gi|109508168
ShhC	CHAPS	FASN	gi|56133
ShhC	CHAPS	neurestin alpha [Rattus norvegicus]	gi|9910320
ShhC	CHAPS	neuroligin 3 [Rattus norvegicus]	gi|19705445
ShhC	CHAPS	Putative alpha-mannosidase C1orf22	gi|109498013
ShhC	CHAPS	Exocyst complex component 4 (Exocyst complex component Sec8) (rSec8)	gi|24418659
ShhC	CHAPS	EH-domain containing 1 [Mus musculus]	gi|7106303

Supplemental Table 2: List of antibodies used in this study. Antibodies used in this study listed in alphabetical order of common name, with species, antibody #, source, and application also indicated. WB = western blot, ICC = immunocytochemistry, IHC = immunohistochemistry.

Antigen	Species	Antibody #	Source	Application	Dilution
Calnexin	Rabbit	ab22595	Abcam	ICC	1:200
c-Myc tag	Mouse	9E10 (sc-40)	Santa Cruz Biotech	WB/ICC	1:1000/1:200
EEA1	Rabbit	ab2900	Abcam	ICC	1:200
GAPDH	Mouse	6C5 (ab8245)	Abcam	WB	1:5000
GFP	Goat	600-101-215	Rockland Inc	WB	1:1000
GFP	Rabbit	A11122	Life Technologies	ICC/IHC	1:1000
HA tag	Rabbit	Y11 (sc-805)	Santa Cruz Biotech	ICC	1:200
Lamp1	Rabbit	ab24170	Abcam	ICC	1:200
Pax2	Goat	PRB-276D	Covance	IHC	1:200
ShhN	Rabbit	H-160 (sc-9024)	Santa Cruz Biotech	WB/ICC	1:1000/1:200
ShhN (mature)	Mouse	5E1	Dev. Studies Hybridoma Bank	ICC	1:5000
Sortilin	Rabbit	ab16640	Abcam	WB/ICC	1:1000/1:200
SV2	Rabbit	119002	Synaptic Systems	ICC	1:200
Tau	Rabbit	314002	Synaptic Systems	ICC	1:5000
TGN-38	Mouse	sc-271624	Santa Cruz Biotech	ICC	1:200
GRP78	mouse	610979	BD Biosciences	WB	
GS28	mouse	611184	BD Biosciences	WB	
SHH	rabbit	Sc-9024	Santa Cruz	WB	
Sortilin	mouse	612101	BD Biosciences	WB	
Vti1b	mouse	611405	BD Biosciences	WB	